Research Square

Preprints are preliminary reports that have not undergone peer review.
They should not be considered conclusive, used to inform clinical practice,
or referenced by the media as validated information.

PIN-FORMED (PIN) gene family in cultivated strawberry (Fragaria x ananassa): Genome-wide characterization and expression profiling under different abiotic stresses and hormonal treatments

Jeba Faizah Rahman
Chattogram Veterinary and Animal Sciences University, Chattogram-4330, Bangladesh
https://orcid.org/0009-0005-3078-7312

Md. Hammadul Hoque
hammadul-geb@sust.edu
Shahjalal University of Science and Technology, Sylhet-3114, Bangladesh https://orcid.org/0000-0001-6613-8510

Md. Nazmul Hasan
Daffodil International University, Dhaka-1216, Bangladesh

Z. M. Tauhidul Islam Shijan
Shahjalal University of Science and Technology, Sylhet-3114, Bangladesh

Mahmudul Hasan
Shahjalal University of Science and Technology, Sylhet-3114, Bangladesh

Md. Abunasar Miah
Noakhali Science and Technology University, Noakhali-3814, Bangladesh.

Shamsul H. Prodhan
Shahjalal University of Science and Technology, Sylhet-3114, Bangladesh

Research Article

Keywords: Cultivated strawberry, Auxin-efflux transporters, PIN-FORMED (PIN) gene family, Protein structure, Abiotic stress response, Gene expression analysis

Posted Date: June 23rd, 2026

DOI: https://doi.org/10.21203/rs.3.rs-10096056/v1

License: This work is licensed under a Creative Commons Attribution 4.0 International License.
Read Full License

Additional Declarations: The authors declare no competing interests.

PIN-FORMED (*PIN*) gene family in cultivated strawberry (*Fragaria x ananassa*): Genome-wide characterization and expression profiling under different abiotic stresses and hormonal treatments

Jeba Faizah Rahman[1], Hammadul Hoque[2,*], Md. Nazmul Hasan[3], Z. M. Tauhidul Islam Shijan[2], Mahmudul Hasan[2], Md. Abunasar Miah[4], and Shamsul H. Prodhan[2]

[1]Department of Bioprocess and Genetic Engineering, Chattogram Veterinary and Animal Sciences University, Chattogram-4330, Bangladesh

[2]Department of Genetic Engineering and Biotechnology, Shahjalal University of Science and Technology, Sylhet-3114, Bangladesh

[3]Department of Genetic Engineering and Biotechnology, Daffodil International University, Dhaka-1216, Bangladesh

[4]Department of Biotechnology and Genetic Engineering, Faculty of Biological Sciences, Noakhali Science and Technology University, Noakhali-3814, Bangladesh.

*Corresponding Author

E-mail: hammadul-geb@sust.edu

Abbreviations: PIN, PIN-FORMED; CREs, *cis*-regulatory elements; PEG, polyethylene glycol; NAA, 1-Naphthaleneacetic acid; IAA, Indole-3-acetic acid; GA_3, Gibberellic acid; RT-qPCR, reverse transcription quantitative polymerase chain reaction; h, hour; d, day;

Abstract

The *PIN-FORMED (PIN)* gene family encodes auxin-efflux carriers that plays a central role in directional auxin gradients in plants. Cultivated strawberry (*Fragaria x ananassa*) is a commercially important fruit crop valued for its nutritional quality and high consumer demand. However, there is no comprehensive analysis of the *PIN* gene family in cultivated strawberry. This study identified thirty *FaPIN* genes. The phylogenetic analysis classified them into five distinct groups. Identifying potential CREs in their promoter region has unveiled their involvement in cellular-development, hormonal-regulation, and stress control. Expression profiling using RT-qPCR demonstrated their differential expression under various abiotic stress conditions. *FaPIN3*,

4, 18 showed significant upregulation under drought; *FaPIN4, 25* under salt, and *FaPIN16* under heat stress. In addition, hormonal treatments revealed distinct tissue-specific expression patterns, with significant upregulation in roots. Collectively, these results indicate that *FaPIN* genes are involved in multiple aspects of stress adaptation and hormone-regulated development in cultivated strawberry.

Keywords: Cultivated strawberry, Auxin-efflux transporters, PIN-FORMED (PIN) gene family, Protein structure, Abiotic stress response, Gene expression analysis.

1. Introduction

Auxin is a crucial phytohormone that functions as a significant signaling molecule and its ability to regulate fundamental processes such as cell division, elongation, differentiation, organ formation and tropic responses (Perrot-Rechenmann 2010, Velasquez, Barbez et al. 2016, Marhava, Bassukas et al. 2018, Braybrook 2019) underscores its role as a key determinant of plant growth and development (Vanneste and Friml 2009). From the earliest stages of embryogenesis to the establishment of the mature plant architecture, auxin coordinates growth and differentiation in a highly regulated manner (Teale, Paponov et al. 2006, Zhao 2010, Robert, Park et al. 2018, Manna, Rengasamy et al. 2022). Auxin concentration gradient and its asymmetric distribution across plant tissues is maintained by a directional transport system known as polar auxin transport (PAT) which is tightly regulated and coordinated by a network of influx and efflux transporters (Grones and Friml 2015, Kumar, Kherawat et al. 2021). There are three principal auxin transporter families involved in polar auxin transport (PAT) between cells: PIN-FORMED (PIN) proteins and ATP-Binding Cassette (ABC) transporters responsible for auxin efflux, and AUXIN RESISTANT1 (AUX1)/AUX1-LIKE (LAX) proteins for auxin influx (Monroy-González, Uc-Chuc et al. 2023).

The *PIN-FORMED (PIN)* gene family encodes plant-specific auxin efflux carriers that are essential for the establishment of auxin gradients (Adamowski and Friml 2015). They are integral membrane proteins with a conserved structural organization which consists of two hydrophobic domains, each containing five transmembrane helices that anchor the protein in the membrane, separated by a central hydrophilic loop that contributes to functional diversification (Křeček,

Skůpa et al. 2009, Ung, Winkler et al. 2022). The hydrophilic loop exhibits significant variability across PIN family members and serves as a regulatory domain that plays a role in phosphorylation, protein-protein interactions, and intracellular trafficking, thus aiding in functional diversification. The asymmetric localization of PINs at the plasma membrane determines the direction of auxin flow between cells and tissues, facilitating upward, downward, or lateral transport depending on developmental and environmental cues (Wisniewska, Xu et al. 2006). Shorter variants of PIN, characterized by diminished hydrophilic loops, are found in the endoplasmic reticulum, where they play a crucial role in regulating intracellular auxin homeostasis. This modular structure allows PIN proteins to manage auxin distribution at both the tissue and cellular levels and through differential expression patterns and subcellular localization, PINs have been shown to regulate vascular patterning, root system architecture, shoot branching, and reproductive development (Blilou, Xu et al. 2005, Vieten, Sauer et al. 2007, Petrášek and Friml 2009).

Beyond their developmental functions, *PIN* genes have emerged as important regulators in stress responses. Under adverse environmental conditions, altered *PIN* expression and re-localization drive auxin redistribution that modulates root system architecture, leaf morphology, and other adaptive traits. For instance, PIN-dependent auxin flux has been linked to drought-induced stomatal regulation, salt-induced root gravitropism and cold-responsive changes in root growth dynamics (Shibasaki, Uemura et al. 2009, Wang, Chai et al. 2015, Kumar, Kherawat et al. 2021). Moreover, auxin transport is integrated into hormonal crosstalk that balances growth and stress tolerance by *PIN*s' interactions with abscisic acid, jasmonic acid, ethylene, and cytokinin. (Wang, Hu et al. 2009, Zhao 2010, Gou, Nai et al. 2022). This integration highlights the significance of the PIN protein as a crucial regulator at the intersection of growth and environmental adaptation.

PIN gene family have been documented thus far in a variety of species (Viaene, Delwiche et al. 2013). The number of *PIN* genes shows considerable variation ranging from very few in *Marchantia polymorpha* (4) (Bennett, Brockington et al. 2014) and papaya (6) (Estrella-Maldonado, Fuentes Ortiz et al. 2016), to moderate in *A. thaliana* (8) (Křeček, Skůpa et al. 2009, Bennett, Brockington et al. 2014), grapevine (12) (Gou, Nai et al. 2022), pepper (10) (Zhang, Dong et al. 2018), tomato (10) (Pattison and Catalá 2012), watermelon (11) (Yu, Dong et al. 2017), and rice (12) (Miyashita, Takasugi et al. 2010, Manna, Rengasamy et al. 2022). On contrast certain species such as maize (15) (Yue, Tie et al. 2015), cotton (17) (He, Zhao et al. 2017, Zhang, He et

al. 2017), and soybean (23) (Liu and Wei 2017) notably possess larger *PIN* gene families. As PIN proteins play a crucial role in regulating the spatial distribution of auxin within plants, they represent a vital focus for research aimed at understanding plant growth and developmental processes.

The cultivated strawberry (*Fragaria* × *ananassa*) is an allo-octoploid (2n=8x=56) species that originated from the hybridization between the Chilean strawberry (*F. chiloensis*) and the North American wild strawberry (*F. virginiana*). Subsequent domestication and selective breeding have produced *F.* × *ananassa* varieties yielding large, flavorful fruits, making it commercially significant and extensively cultivated fruit crops worldwide (Njuguna, Liston et al. 2013). The sequencing of the diploid ancestor*, F. vesca* in 2010 (Shulaev, Sargent et al. 2011) marked a major advancement, providing a valuable genetic reference for marker development and trait association studies within *Fragaria* species (Anciro, Mangandi et al. 2018). Recently, a new reference genome for *F.* ×*ananassa* was established, shedding light on the intricate evolutionary origins of octoploid strawberries(Edger, Poorten et al. 2019). This updated genome sequence represents an essential resource for understanding the octoploid strawberry's genetic complexity. It will specifically improve the functional annotation of important regulatory gene families and systematic, genome-wide studies.

The functions of the *PIN* gene family are well-documented in model plants; however, their functions in strawberry development and stress adaptation are still inadequately explored. The significance of auxin-driven signaling in growth and stress responses necessitates a thorough analysis of the *PIN* gene family in strawberry. This study involved a comprehensive analysis of *PIN* genes in strawberry, along with their characterization, structural characteristics, evolutionary relationships, and expression patterns. Expression profiling was performed under phytohormone treatments and abiotic stress settings to clarify the roles of *PINs*. These findings aim to enhance our understanding of auxin-driven signaling in strawberry and provide candidate genes for breeding strategies to enhance stress resilience and fruit quality.

2. Materials and methods

2.1 Screening of *PIN* gene family in the *F.* ×*ananassa* genome and their characterization

In order to identify strawberry PIN proteins, a BLASTP search was conducted using *Arabidopsis thaliana* PIN protein sequences as queries against the *Fragaria x ananassa v1.0.a1* genome dataset available in the Phytozome v13 database (https://phytozome-next.jgi.doe.gov/info/Fxananassa_v1_0_a1) (Goodstein, Shu et al. 2012). TAIR database (https://www.arabidopsis.org/) (Lamesch, Berardini et al. 2012) was employed to retrieve the protein sequence of eight AtPINs (AT1G73590, AT5G57090, AT1G70940, AT2G01420, AT5G16530, AT1G77110, AT1G23080, and AT5G15100) (Křeček, Skůpa et al. 2009). These AtPIN protein sequences were also used in independent BLASTP searches within the NCBI Protein database (https://www.ncbi.nlm.nih.gov/protein) to guarantee complete identification. To confirm the existence of the distinctive transmembrane domains, all candidate members were further investigated in the TMHMM v.2.0 web server (https://services.healthtech.dtu.dk/services/TMHMM-2.0/) (Krogh, Larsson et al. 2001). Additionally, the Pfam (http://pfam.xfam.org/) (Mistry, Chuguransky et al. 2021) and NCBI conserved domain database (https://www.ncbi.nlm.nih.gov/Structure/cdd/wrpsb.cgi) (Lu, Wang et al. 2020) were employed to confirm the conserved domains characteristics of PIN proteins, including the conserved N- and C- terminal transmembrane regions. The domain organization *FaPIN* genes was predicted using the HMMER web server (hmmscan tool) with default parameters against the Pfam database (Potter, Luciani et al. 2018).

Any sequence lacking the characteristic PIN transmembrane architecture were excluded from further analysis. The validated proteins were named as 'FaPIN', where 'Fa' prefix denotes *Fragaria x ananassa*. They were sequentially numbered based on their chromosomal order, arranged from the upper to the lower regions of each chromosome, in accordance with previously established naming conventions (Tapia, Barbey et al. 2020, Tian, Xu et al. 2024). Details such as locus IDs, strand orientation, coding sequence coordinates (5′-3′ direction), gene lengths and CDS lengths for the identified genes were retrieved from the Phytozome v13 database (https://phytozome-next.jgi.doe.gov/) (Goodstein, Shu et al. 2012). To determine the corresponding proteins' physicochemical properties, such as their theoretical isoelectric point and molecular weight, the ExPASy ProtParam tool (https://web.expasy.org/protparam/) (Gasteiger, Hoogland et al. 2005) was utilized. Then their subcellular localization was predicted employing CELLO v.2.5 (http://cello.life.nctu.edu.tw/) (Yu, Chen et al. 2006) and WoLF PSORT (https://www.genscript.com/wolf-psort.html) (Horton, Park et al. 2007) web tools. Additionally,

to examine sequence similarity among *FaPINs* proteins, a multiple sequence alignment was done in MEGA X (Kumar, Stecher et al. 2018). The ClustalW algorithm was applied using its default settings and the alignment results were visualized using GeneDoc version 2.7 (Nicholas 1997) software.

2.2 Phylogenetic analysis

The complete amino acid sequence of the thirty FaPIN proteins were used for phylogenetic analysis. With 1000 bootstrap replicates to ensure statistical reliability and the Maximum-likelihood approach, an unrooted phylogenetic tree was built in MEGA X (Kumar, Stecher et al. 2018). The complete PIN protein sequences from *Arabidopsis* (Křeček, Skůpa et al. 2009), rice (Manna, Rengasamy et al. 2022) and woodland strawberry were utilized to explore the evolutionary relationships of PIN proteins among different plant species. The rice PIN protein sequences were downloaded from Phytozome, while the FvPIN sequences of woodland strawberry was collected from NCBI (https://www.ncbi.nlm.nih.gov/). Then an unrooted phylogenetic tree was generated using MEGA X based on these sequences, applying Maximum-likelihood approach with 1000 bootstrap replicates. The resulting tree classified the FaPIN proteins into distinct groups. Final tree annotation, editing and visualization were carried out using iTOL (https://itol.embl.de/) (Letunic and Bork 2007) web tools.

2.3 Gene structure and conserved motif analysis of *FaPIN*s

The exon-intron architecture of the *FaPIN* gene family was examined using the Gene Structure Display Server (GSDS 2.0; https://gsds.gao-lab.org/) (Hu, Jin et al. 2015). Further, to identify the conserved motifs within the FaPIN proteins, the MEME suite (version 5.4.0; https://meme-suite.org/meme/tools/meme) (Bailey and Elkan 1994) was employed. All analyses were conducted with default settings, except that the maximum number of detectable motifs was limited to 15.

2.4 Chromosomal mapping

To visualize the chromosomal positioning of *FaPIN* genes within the octoploid strawberry genome, their physical locations were mapped using MapChart software (Voorrips 2002). The mapping was done using the gene coordinate data from the Phytozome database, particularly the CDS data given in Table 1.

2.5 *Cis*-regulatory elements (CREs) analysis

Using the PlantCARE database (https://bioinformatics.psb.ugent.be/webtools/plantcare/html/) with default settings, a 1.5 kb sequence upstream of the ATG start codon was screened for potential *cis*-regulatory elements within the promoter regions of *FaPINs* (Lescot, Déhais et al. 2002). The resulting *cis*-elements were grouped according to their biological roles. TBtools software was then utilized to visualize important CREs related to hormone regulation, developmental regulation, and responses to biotic and abiotic stresses (Chen, Chen et al. 2020).

2.6 Structure analysis of FaPIN proteins

For secondary and tertiary stricture analysis, eleven FaPIN proteins were chosen from the thirty members based on their phylogenetic classification and number of predicted transmembrane helices.

Secondary structure prediction of eleven FaPIN proteins was carried out using STRIDE (https://webclu.bio.wzw.tum.de/stride/) (Heinig and Frishman 2004) under default conditions, highlighting the proportions of turns, coils, 3_{10} helices, α-helices and β-sheets in distinct colors.

For tertiary structure prediction, the RoseTTAFold algorithm was applied on the Robetta server (https://robetta.bakerlab.org/) (Kim, Chivian et al. 2004). The preliminary models were further refined through the GalaxyRefine platform (https://galaxy.seoklab.org/cgi-bin/submit.cgi?type=REFINE)(Ko, Park et al. 2012) and subjected to energy minimization using Swiss-PdbViewer v4.1(https://spdbv.unil.ch/) (Guex and Peitsch 1997). Model validation was carried out with PROCHECK (Laskowski, Rullmann et al. 1996) and ERRAT (Colovos and Yeates 1993) via the SAVES server (https://saves.mbi.ucla.edu/), while ProSA-web (https://prosa.services.came.sbg.ac.at/prosa.php) (Wiederstein and Sippl 2007) provided Z-scores. The finalized 3D models were then visualized using Biovia Discovery Studio (Biovia 2017).

2.7 Plant samples, stress treatments and total RNA extraction

In this study, a cultivated variety of *F. x ananassa* was used as experimental material. Germinated seedlings were obtained from the Bangladesh Agricultural Research Institute (BARI), and only vigorous, disease-free plants were selected as explants for subsequent treatments. The seedlings were maintained in a greenhouse under controlled conditions- 22°C temperature, 70% relative

humidity, and natural light using plastic pots (14 cm in diameter and 10 cm in height). After one month of growth, the plants were subjected to various abiotic stress treatments, including drought (3mg/L PEG), heat (42° C), cold (4° C), and salinity (300 mM NaCl). Hormonal treatments involved the application of IAA (1mg/L), NAA (0.3mM) and GA (0.1mM). each condition maintained for 24 hours. Untreated plants served as control. Leaf samples were collected at 24 hours post-treatment, while root tissues were also harvested to assess gene expression under hormonal exposure. Fresh tissues were flash-frozen in liquid nitrogen and preserved at -80° C. before RNA extraction, all samples were washed thoroughly with (RNAase free) distilled water and 70% ethanol to remove contaminants.

Total RNA extraction was performed according to the method described in (Hazman, Kabil et al. 2020) utilizing the Invitrogen ™ TRIzol™ reagent (Thermo Fisher Scientific, USA) to remove residual genomic DNA, samples were treated with DNase I using the Invitrogen™ DNA-free™ DNA Removal Kit (Thermo Fisher Scientific, USA). Complementary DNA (cDNA) was then synthesized from the purified RNA using the GoScript™ Reverse Transcription System (Promega Corporation, USA). All steps were carried out in strict adherence to the respective manufacturer's instructions.

2.8 RT-qPCR analysis and expression profiling of *FaPIN* genes under abiotic stress and hormonal treatments

Through RT-qPCR, ten *FaPIN* genes (*FaPIN3, FaPIN4, FaPIN11, FaPIN13, FaPIN14, FaPIN16, FaPIN18, FaPIN25, FaPIN27 and FaPIN29*) were used for expression profiling under several abiotic stress and hormones. The genes were chosen based on their phylogenetic groups.

Primers used for RT-qPCR analysis (listed in Table S5) were designed using NCBI Primer BLAST (https://www.ncbi.nlm.nih.gov/tools/primer-blast/) (Ye, Coulouris et al. 2012) and verified for quality parameters through the OligoAnalyzer Tool from Integrated DNA Technologies, Inc. (https://sg.idtdna.com/pages/tools/oligoanalyzer). Real time PCR assays were carried out using the Bio-Rad CFX96^{TM} Real-Time PCR Detection System with the GoTaq® qPCR Master Mix (2X) from Promega Corporation (USA). The eukaryotic elongation factor eEF-1α served as the internal reference gene (Jain, Nijhawan et al. 2006). Each 15 µL reaction consisted of 7.5 µL GoTaq® qPCR Master Mix (2X), 1 µL of each gene-specific primer, 2 µL of cDNA (diluted tenfold), and 3.5 µL of nuclease free water. The thermal cycling protocol was 10 min initial denaturation at

95°C, followed by 40 cycles of 95°C for 15 s, annealing for 30 s, and extension at 72°C for 40 s. Three separate experiments were performed on each sample, and melting curve analysis was conducted to verify amplification specificity.

The $2^{\wedge-\Delta\Delta Ct}$ method was used to calculate relative gene expression(Livak and Schmittgen 2001). To determine the average expression value among the different treatments, technical replication was used. Statistical analysis was performed using Microsoft Office 2019 and GraphPad Prism 9.00 (Motulsky 1999). One-way ANOVA followed with Bonferroni post hoc tests was applied for stress treatments, while two-way ANOVA followed by Bonferroni correction was used for hormone treatments. Significant differences ($P \leq 0.05$) were denoted with varying levels of asterisks.

3. Results

3.1 Identification and characterization of the *PIN-FORMED (PIN)* gene family in *F. x ananassa*

A total of thirty *PIN-Formed (PIN)* genes were identified in *Fragaria x ananassa*. Initial BLASTP searches were conducted using AtPIN protein sequences as queries against the *F. x ananassa* genome yielding 41 potential matches. These 41 transcripts were then subjected to domain validation. Among them, 30 transcripts were confirmed to contain the characteristic transmembrane domain architecture of the PIN proteins, indicating that *Fragaria x ananassa* harbors 30 distinct PIN genes, each represented by a single transcript with no alternative splice form. To ensure completeness, an additional BLASTP search was performed against the NCBI protein database, which confirmed that all putative *PIN* genes had been selected. The 30 genes were named *FaPIN1* through *FaPIN30*, based on their physical locations on the chromosomes. Conserved domain organization of the thirty FaPIN proteins predicted using HMMER web server's hmmscan tool against Pfam are detailed in Table S2. Transmembrane helix prediction through TMHMM v.2.0 indicated that most FaPIN proteins possess between six and nine helices, while FaPIN2, 3, 4, 15, 17 and 21 were found to have five helices. Structurally, all FaPIN proteins shared a common layout- conserved transmembrane domains at both N- and C- termini anchoring the protein in the membrane, and a central hydrophilic loop oriented toward the cytoplasm. The predicted transmembrane helices are shown in Figure 1.

According to sequence analysis, the deduced proteins had lengths ranging from 313 to 1247 amino acids, and the lengths of the gene and CDS varied from 942 bp (*FaPIN4*) to 13627 bp (*FaPIN9*) and 942 bp (*FaPIN4*) to 3744 bp (*FaPIN9*), respectively. These proteins exhibited varying sizes. With 1247 amino acids in length and a molecular weight (MW) of 130.05 kDa, *FaPIN9* encodes the largest protein in the family; in contrast, *FaPIN4* is the smallest, with 313 amino acids in length and a MW of 35.01 kDa. Moreover, the protein's predicted isoelectric points (pI) varied from 5.04 (*FaPIN21*) to 9.84 (*FaPIN2*). The proteins exhibited an average MW of about 57.81 kDa and a pI of about 8.09. The FaPIN proteins are probably localized to the plasma membrane and a few can be found in vacuoles also, according to subcellular localization analysis. Table 1 lists all of the representative *FaPIN* genes' comprehensive physicochemical characteristics. Multiple sequence alignment also revealed strong conservation within the N- and C-terminal transmembrane domains, which are characteristic of PIN transporters, while the central hydrophilic loop showed greater sequence variability (Figure S1).

3.2 Phylogenetic analysis

The FaPIN proteins were categorized into five groups (I-V) based on their phylogenetic analysis with *Oryza sativa*, *Arabidopsis thaliana* and *Fragaria vesca* PIN proteins, highlighting both conservation and diversification across species (Figure 2). FaPIN1, 2, 3, 4, 5, 6, 11, 12, 14, 15 are in Group I. FaPIN7, 8, 10 and 13 are in Group II. Group III includes FaPIN20, 24, 25, 30 and Group IV includes FaPIN22, 23, 27 and 28. Group V includes FaPIN16, 17, 18, 19 26 and 29. Each clade contained FaPINs as well as PIN members from the model species *Arabidopsis* and rice which suggests evolutionary conservation across monocots and dicots.

Group V included FaPINs clustered with AtPIN1 and multiple rice OsPIN1 paralogs, which have been reported to mediate polar auxin transport in vascular tissues and organ patterning (Wang, Hu et al. 2009, Li, Zhu et al. 2019, Manna, Rengasamy et al. 2022). Group I contained FaPINs closely related to AtPIN2,3 which are recognized in Arabidopsis for their role in regulating root development and tropic responses (Friml, Wiśniewska et al. 2002, Retzer, Akhmanova et al. 2019), while Group II included FaPINs alongside AtPIN4,7 which are linked to embryogenesis and meristem function (Blilou, Xu et al. 2005). Members of Group III clustered with AtPIN8 and rice reflecting conserved functions in reproductive and organ development. In contrast, Group IV contained FaPINs related to AtPIN5, 6 which are primarily involved in intracellular auxin

regulation. The widespread presence of FaPINs across various clades indicates both evolutionary conservation and gene expansion in octoploid strawberry, implying functional diversification to support its complex developmental processes.

3.3 Gene structure and conserved motif analysis

The structural diversity of exons and introns is a key factor influencing gene family evolution. Gene structure analysis revealed that most members of *FaPIN* gene family had five introns and six exons in common, except for *FaPIN 3, 21, 1, 9, 17, 22, 23, 27* and *28* (Figure 3). In addition, *FaPIN2* and *4* do not have any intron. This intron-exon structure indicated that they were related in an evolutionary way.

To investigate the distribution and diversity of conserved motifs within the FaPIN proteins of *Fragaria x ananassa*, the MEME web server (Bailey and Elkan 1994) was employed. This analysis revealed 15 distinct conserved motifs, which are sequentially numbered from Motif 1 to Motif 15 (Figure 4). As expected for members of the PIN family, several motifs were highly conserved, reflecting their role in PIN structure and function. Specifically, motifs 1, 2, 3, 11 and 14 were present in all FaPIN proteins, consistent with their conservation in model species such as *Arabidopsis thaliana* and *Oryza sativa*, where these motifs are critical for auxin transport activity and membrane localization (Paponov, Teale et al. 2005). In contrast, some motifs exhibited variable distribution, suggesting potential functional divergence within the FaPIN family. For example, motif 5 and 7 were found in all proteins except FaPIN 24, 30, 20, 25, 22, 23, 27 and 28 while motif 15 was present in FaPIN2, 1, 9, 15, 6, 12, 14, 8, 13, 7 and 10. Similarly, motif 9 was absent in multiple proteins (FaPIN 3, 21, 2, 4, 1, 30, 20, 25, 22, 23, 27, 28) and motif 10 was absent in 3, 5, 26, 29, 24, 30, 20, 22, 23, 25, 27, 28. By contrast, motif 12 appeared in multiple proteins (FaPIN 9, 15, 5, 11, 6, 12, 14, 8, 13. 7, 10, 16, 18, 17, 19), whereas motif 4 and 8 were missing in only a few proteins (FaPIN 3, 21, 2, 4, 1, 15, 17). Motif 6 were absent in FaPIN3, 21, 2, 4, 1, 15, 5 and motif 13 were absent in FaPIN 3, 21, 2, 4, 1, 9, 15, 5, 16, 8, 17, 19 and 28. The biological roles of these motifs are still unknown and require further investigation and experimental validation for clarification.

3.4 Chromosomal distribution of *FaPINs*

Chromosome distribution analysis revealed that no *FaPIN* genes were located on the third and seventh homologous chromosome sets of *F.* × *ananassa*. In contrast, the remaining six homologous chromosome sets exhibited an uneven distribution of *FaPIN* genes, with the fourth and sixth sets having the highest number of *FaPIN* members.

3.5 Analysis of Cis-regulatory elements (CREs) in the *FaPIN* promoter regions

Cis-regulatory elements play a crucial role in modulating gene transcription. To uncover the potential regulatory factors influencing *FaPIN* gene expression under different conditions, the 1.5kb upstream promoter regions of all *FaPIN* genes were examined using the PlantCARE database. This analysis identified a total of 70 distinct CREs distributed within the 5′ untranslated regions (5′ UTRs) of the *FaPIN* promoters.

These elements were divided into a number of functional groups, such as promoter-related, biotic stress-responsive, hormonally regulated, cellular development, and miscellaneous functions. Furthermore, a few CREs with unclear roles were discovered in the *FaPIN* genes. A comprehensive list of all identified CREs and their putative functions is provided in supplementary Table S2. The abundance of stress-responsive CREs and hormone regulation in the *FaPINs* is shown in Figure 6, highlighting their possible involvement in mediating *FaPIN* gene responses to environmental and endogenous cues.

Among the CREs, elements associated with hormonal regulation were most prominent. Abscisic acid responsive elements (ABRE, ABRE3a, and ABRE4) were widely distributed across many *FaPIN* promoters, especially in *FaPIN1, 7, 13, 18, 19, 22,* and *23*. Gibberellin-responsive motifs (GARE-motif, P-box, CARE, and TATC-box) were also frequently observed in genes such as *FaPIN5, 9, 12, 15, 17, 19* and *27*, suggesting that gibberellin may play a role in modulating *FaPIN* expression. Salicylic acid-responsive elements (TCA-element and TGA-element) were identified in various genes including *FaPIN4, 5, 10,* and *23*, while auxin-responsive elements and those responsive to methyl jasmonate (CGTCA-motif, TGACG-motif and as-1) were also widespread, indicating that multiple hormones signalling pathways influence *FaPIN* regulation. In addition, several CREs linked to cellular development were identified. For instance, the CAT-box, involved in meristem-specific expression was detected in *FaPIN2, 3, 6, 7,* and *14*. Xylem-development associated motifs (such as the AAGAA-motif, AC-II) were highly represented across many *FaPINs,* indicating a possible role in vascular development. Abiotic responsive elements were also

abundant as well. ARE and GC-motif, essential for anaerobic and anoxic stress responses, were present in most *FaPINs*, while LTR elements associated with cold responsiveness appeared in genes like *FaPIN1, 3, 8* and *9*. Motifs such as MBS, MYB, MYC, and DRE which are involved in drought, salinity, and temperature responses, were particularly enriched in *FaPIN6, 18, 21, 28* and *30*, reflecting their potential roles in stress adaptation. CREs responsive to biotic stress were also identified. W-box, WRE3, WUN-motifs, known to mediate responses to pathogens and wounding, were found in genes such as *FaPIN4,7,10,24* and *30*. Light-responsive elements were notably abundant and diverse, including motifs such as Box 4, G-box, GT1-motif, AE-box, ACE, I-box, and TCT-motif. These were present in nearly all *FaPIN* genes, indicating a broad involvement of light in regulating their expression. Additionally, core promoter elements like CAAT-box and TATA-box were found in all *FaPIN* genes, with high frequencies in genes such as *FaPIN12, 22, 23* and *26*, supporting their roles in basal transcription initiation. Overall, this comprehensive CRE profiling highlights the complex regulatory potential of *FaPIN* genes and suggests their involvement in diverse hormonal, developmental and environmental response pathways.

3.6 Protein structure analysis

For protein structure analysis, eleven FaPIN proteins *(FaPIN1, 3, 4, 11, 13, 14, 16, 18, 25, 27 and 29)* were chosen among the thirty identified members based on their phylogenetic classification and the quantity of predicted transmembrane helices.

Secondary structure composition of eleven FaPINs were analyzed to evaluate their structural organization and infer potential functional implications (Figure 7). The percentage composition of each type of secondary structure element is detailed in Table S3. The results showed that α-helices constitute the predominant secondary structure element in all proteins, with proportions ranging from 44.19% (FaPIN1) to 79.83% (FaPIN25). The high abundance of α-helical content suggests that FaPIN proteins possess a compact and stable structure, consistent with their role as transmembrane auxin efflux carriers (Muthukumaran, Manivel et al. 2011). Such α-helix-rich architecture is characteristic of integral membrane proteins (White and Wimley 1999) and typically facilitates membrane integration and directional auxin transport across plant tissues. The coil (loop) content ranged from 7.28% (FaPIN27) to 18.06% (FaPIN29), indicating the presence of flexible segments likely involved in protein-protein interactions, conformational regulation or subcellular localization and a crucial role in signaling cascades (Deng, Sun et al. 2015). The 3_{10}

helix content was comparatively low (ranging from 0-11.36%), while turn structures showed moderate representation (8.68-24.46%), indicating local folding adaptations essential for maintaining the spatial arrangement of transmembrane helices and cytosolic loop. Meanwhile, extended β-strand (β-sheet) elements and isolated β-bridges were found in low abundance (0-7.25%) and 0-1.52%, respectively), suggesting that FaPIN proteins are primarily α-helix-based with minimal β-structure involvement.

Three-dimensional structures of the eleven FaPIN proteins were initially modelled using the RoseTTAFold algorithm available on the Robetta platform (Kim, Chivian et al. 2004). To improve structural accuracy, the preliminary models underwent refinement through GalaxyRefine platform (Ko, Park et al. 2012), followed by energy minimization using SwissPdbViewer (Guex and Peitsch 1997). The finalized tertiary structures were visualized in Discovery studio (Biovia 2017) are presented in Figure 8. Model validation was carried out using multiple quality-assessment tools, including PROCHECK (Laskowski, Rullmann et al. 1996), ERRAT (Colovos and Yeates 1993), and ProSA-web server (Wiederstein and Sippl 2007), with detailed evaluation metrics provided in Table S4. Structural reliability was further confirmed through Ramachandran plot analysis generated by PROCHECK, which verified the stereochemical quality of the modeled proteins. The quality of the proteins was assessed through the PROCHECK's Ramachandran plot analysis. The analysis revealed that majority of residues in each FaPIN model occupied energetically favorable conformations (Figure S2). Specifically, 88.7% to 91.8% of residues were found in the most favored regions, while 6.0% to 9.6% were located in the additionally allowed regions. A small fraction (≤1.5%) appeared in generously allowed regions, and only 0.4% to 1.7% of residues were located in disallowed regions, indicating minimal conformational strain. These results suggest that the predicted protein structures possess acceptable stereochemical quality, with no significant backbone geometry anomalies. The ERRAT scores (Colovos and Yeates 1993) of the predicted models, which evaluate the quality of non-bonded atomic interactions, ranged from 91.809 to 96.491 (File S1). Since ERRAT values above 90 are generally considered acceptable for high quality homology models, these results indicate that the FaPIN protein structures are structurally reliable and suitable for downstream functional and docking studies. In addition, the ProSA-web server (Wiederstein and Sippl 2007) was used to evaluate the structural quality of the modeled FaPIN proteins by calculating Z-scores, which reflect how closely the predicted structures align with the experimentally determined native proteins (Figure S3). These Z-scores, detailed in Table

S4 ranged from -4.08 to -6.73. Such values fall well within the range typically observed for native proteins of comparable size resolved by X-ray crystallography, supporting the reliability of the models. The most negative Z-scores (e.g., -6.73 for FaPIN1 and -6.68 for FaPIN3) reflect stable protein folds, while the rest are still within acceptable quality thresholds for modeled proteins. These collective outcomes underscore the high standard of the modeled tertiary protein structures.

3.7 Expression analysis of *FaPINs* under various abiotic stresses and hormonal treatments using RT-qPCR

The expression patterns of ten selected *FaPINs* were analyzed in strawberry seedling leaves following exposure to various abiotic stresses including, heat, cold, salt and drought and hormone treatment such as IAA, NAA and GA_3. The ten *FaPIN* genes (*FaPIN3, 4, 11, 13, 14, 16, 18, 25, 27 and 29*) were chosen from the thirty *FaPIN* members based on their phylogenetic grouping and number of predicted transmembrane helices. The relative expression levels, measured after 24 hours of treatment, are illustrated in Figure 9.

As illustrated in Figure 9, members of the *FaPIN* gene family displayed distinct expression responses to various abiotic stresses. Notably, *FaPIN3* exhibited strong upregulation across all stress treatments with the most pronounced induction observed under drought conditions. *FaPIN4* was induced by several stresses, with significant upregulation observed under salt and heat treatments. *FaPIN11* exhibited increased expression under salt, cold and heat conditions but was downregulated during drought. *FaPIN13* showed general upregulation across all stress treatments. *FaPIN14* displayed lower expression under drought and heat. Although *FaPIN16* expression increased under all stresses, a significant elevation was observed under heat stress, whereas *FaPIN18* shown significant upregulation under drought. *FaPIN25* was highly and significantly expressed under salt stress. *FaPIN27* showed a general upregulation across all stress treatments. *FaPIN29* showed downregulation under drought stress. From this analysis, it has been observed that, under drought condition, *FaPIN11* and *29* showed lower expression. Collectively, these results indicate that all *FaPIN* members exhibit diverse expression under distinct abiotic stresses.

Furthermore, RT-qPCR was performed to investigate the expression behavior of *FaPIN* genes under various plant hormones involved in regulating growth and development. The comparative expression levels of *FaPIN* members in leaf and root tissues under various hormonal treatments (control, NAA, IAA and GA_3) are presented as grouped bar graphs in Figure 10. Expression

analysis revealed that the *FaPINs* exhibited tissue-specific variation in response to hormonal treatments. Under control condition, no significant difference was observed in expression between leaf and root tissues. Following NAA treatment, *FaPIN3, 11, 13, 16, 18* and *27* showed a drastic and significant upregulation in root tissues compared to leaf, indicating a strong auxin-responsive induction in roots. IAA treatment also significantly increased expression in roots relative to leaves in *FaPIN4, 11, 14, 18, 25* and *29*, confirming that this gene is responsive to auxin-type hormones. Similarly, GA_3 treatment resulted in significant higher expression of *FaPIN3, 11, 13, 18*, and *27* in roots, suggesting a role of gibberellin signaling in root-specific expression. The data analysis revealed that the application of NAA, IAA and GA_3 significantly enhanced gene expression in roots compared to leaves, suggesting that the *FaPINs* are predominantly responsive to auxin and gibberellin signaling in root tissue.

4. Discussion

The PIN-FORMED (PIN) protein family, unique to plants, encodes auxin-efflux-transporter proteins crucial in generating gradients and controlling auxin distribution for growth, development and stress responses in plants (Blilou, Xu et al. 2005, Wisniewska, Xu et al. 2006, Křeček, Skůpa et al. 2009, Adamowski and Friml 2015) . A substantial amount of research has been dedicated to characterizing its structure and functional roles in *Arabidopsis* (Friml, Wiśniewska et al. 2002, Blilou, Xu et al. 2005, Shibasaki, Uemura et al. 2009, Retzer, Akhmanova et al. 2019), and crop plants- soybean (Wang, Chai et al. 2015), cotton (He, Zhao et al. 2017, Zhang, He et al. 2017), rice (Wang, Hu et al. 2009, Li, Zhu et al. 2019), wheat (Kumar, Kherawat et al. 2021), maize (Yue, Tie et al. 2015) papaya (Estrella-Maldonado, Fuentes Ortiz et al. 2016), grapevine (Gou, Nai et al. 2022), tomato (Pattison and Catalá 2012), pepper (Zhang, Dong et al. 2018) etc.

The cultivated strawberry possesses a highly complex genome derived from multiple ancestral lineages. The release of a high-quality reference genome of *F. x ananassa* has opened new avenues for exploring the gene families (Edger, Poorten et al. 2019). The present study conducted a comprehensive genome-wide analysis of the *PIN* gene family in *F. x ananassa*, aiming to uncover their evolutionary patterns and possible involvement in auxin-regulated processes governing growth, development, and stress response.

Total thirty *FaPIN* genes were found and all the FaPIN proteins shared the characteristic transmembrane domains at the N- and C-termini and a central hydrophilic cytoplasmic loop

(Křeček, Skůpa et al. 2009) . variations in sequence length, molecular weight, GRAVY scores, and isoelectric points among these genes reflects the structural and physicochemical diversity within the *FaPIN* gene family. Subcellular localization was predicted by two different tools and there are some differences. It has been found that the proteins were localized in plasma membrane and vacuoles. According to WoLF PSORT's (Horton, Park et al. 2007) findings, all the FaPIN proteins are located in plasma membrane. However, CELLO (Yu, Chen et al. 2006) suggests that certain FaPIN proteins (FaPIN20, 22, 23, 24, 27, 28 and 30) may be present in both vacuoles and plasma membrane.

Transmembrane (TM) helices prediction revealed that most FaPIN proteins contain six to nine transmembrane helices, except FaPIN2, 3, 4, 15, 17, and 21, which possess five. Furthermore, a sequence alignment of the thirty FaPIN proteins revealed that they contain highly conserved residues, especially in the N- and C-terminal transmembrane domains whereas the hydrophilic loop exhibits notable sequence divergence, suggesting potential difference in regulatory function. These finding aligns with the conserved structural organization of this protein reported in other plants (Křeček, Skůpa et al. 2009, Bennett, Brockington et al. 2014, Ung, Winkler et al. 2022). Proteins with fewer helices such as AtPIN5, 6 and 8 in *Arabidopsis*, OsPIN5b and OsPIN5c in rice, VvPIN5 in grapevine and TaPIN5-like in wheat, are found to regulate intracellular auxin homeostasis and stress adaptation (Blilou, Xu et al. 2005, Wang, Hu et al. 2009, Kumar, Kherawat et al. 2021, Gou, Nai et al. 2022, Manna, Rengasamy et al. 2022). Conversely, proteins with eight to ten helices, such as AtPIN1-3, OsPIN1b and TaPIN9, are generally localized in the plasma membrane and play crucial role in directional auxin flow for organ development and tropic responses (Wang, Hu et al. 2009, Ganguly, Lee et al. 2010, Miyashita, Takasugi et al. 2010, Kumar, Kherawat et al. 2021). So, the presence of 5 to 9 transmembrane helices among strawberry FaPIN proteins indicates structural and functional diversification, implying that some members likely modulate intracellular auxin balance, whereas others participate in intercellular transport, growth and stress adaptation. Additionally, the degree of conservation also highlights both evolutionary stability of core transporter motifs and functional diversification within the FaPIN gene family.

Evolutionary relationships of PIN proteins across *F. x ananassa*, *Oryza sativa*, *Arabidopsis thaliana* and *Fragaria vesca* (Woodland strawberry) is observed in the phylogenetic tree. The

FaPINs were categorized into five distinct groups (I-V). Group I encompassed FaPIN1-6, 11, 12, 14, 15; Group II contained FaPIN7, 8, 10, 13; Group III comprised FaPIN20, 24, 25, 30; Group IV included FaPIN22, 23, 27, 28; and Group V consisted of FaPIN16-19, 26, 29. Every clade included FaPINs alongside PIN members from model species *Arabidopsis* and rice, indicating evolutionary conservation across monocots and dicots.

Intron–exon structure variation in plant genes is a key driver of evolutionary adaptation (Koralewski and Krutovsky 2011). Gene structure analysis showed that most *FaPIN* genes have five introns and six exons, except *FaPIN1, 3, 9, 17, 21-23, 27, 28*. *FaPIN2* and *4* don't have any introns. The absence of introns in certain genes indicates their high expression levels and suggests that these genes are evolutionarily conserved rather than recently evolved (Deshmukh, Sonah et al. 2016, Nagar, Kumar et al. 2020).

Protein function and specificity depend significantly on conserved motifs (MacIsaac and Fraenkel 2006). Conserved motif analysis found 15 motifs. Most of the motifs were common in the FaPIN proteins of the five phylogenetic groups. From the analysis it was also observed that several motifs were highly conserved, reflecting their role in PIN structure and function. Specifically, Motif 1-3, 11 and 14 were present in all FaPIN proteins. In contrast, the other motifs exhibited variable distribution, indicating potential functional divergence within FaPIN family. The functional roles of the identified motifs remain unexplored at this stage. However, the other motifs showed variable distribution, suggesting functional divergence within the FaPIN family.

Chromosomal distribution shows the random and uneven distribution of the *FaPIN* genes across the seven sets of homologous chromosomes. *FaPINs* were absent in the third and seventh sets of homologous chromosomes of *F.* × *ananassa* and unevenly distributed across the remaining six. The fourth and sixth sets of homologous chromosomes contained the highest number of *FaPIN* genes.

Cis-regulatory elements interact with transcription factors (TFs) to organize the transcription initiation complex, which in turn recruits and activates RNA polymerase, leading to the onset of gene transcription (Sutoh and Yamauchi 2003, Marand, Eveland et al. 2023). A total of 70 distinct CREs were found across the *FaPIN* gene family. These CREs were categorized into seven major functional groups, each playing key roles in transcriptional regulation of gene expression under various physiological and environmental conditions. This analysis highlights the diverse

regulatory landscape of FaPIN gene promoters, suggesting their complex and multifactorial control in response to developmental cues, phytohormones, biotic and abiotic stresses.

The proportions of α-helix, β-sheet, isolated β bridge, turn, coil, and 3_{10}-helix in the eleven FaPIN proteins were revealed by secondary structure analysis. This prediction demonstrates that FaPIN proteins are mainly composed of α-helical domains interspaced with short loops and turns, a structural configuration well-suited for their function in polar auxin transport and subcellular trafficking within plant cells. This observation aligns with previously characterized PIN transporters in Arabidopsis thaliana and other plant species, which possess a typical α-helical transmembrane topology with minimal β-sheet content and exhibit a hydrophobic core comprising multiple α-helical transmembrane segments flanked by a hydrophilic central loop for regulation, trafficking and interaction with other cellular components (Křeček, Skůpa et al. 2009, Adamowski and Friml 2015, Ung, Winkler et al. 2022).

3D structures of eleven FaPIN proteins were predicted and validated by different tools in this study. The structural validation of FaPIN proteins confirmed that the predicted 3D models are accurate and exhibit high-quality conformations. High percentages of residues in favoured regions of Ramachandran plot, strong ERRAT scores and acceptable Z-scores collectively support their structural integrity. These results suggest a conserved structural organization among PIN proteins across plant species, consistent with their role in directional auxin transport (Křeček, Skůpa et al. 2009, Adamowski and Friml 2015, Ung, Winkler et al. 2022). These findings also indicate that the predicted models are suitable for downstream analyses such as functional annotations and molecular docking.

The expression levels of ten *FaPIN* genes were analysed by RT-qPCR in strawberry seedlings under different abiotic stresses (heat, cold, salt, drought) and hormone treatments (IAA, NAA, GA_3). The expression profiling of *FaPIN* genes demonstrated distinct responses to various abiotic stresses. Several members, e.g. *FaPIN3, 4, 13, 16, 18, 25,* and *27*, exhibited significant upregulation under a variety of stress conditions. *FaPIN3* and *FaPIN18* were particularly responsive to drought, while *FaPIN25* was highly induced by salt stress. Conversely, *FaPIN11, 14*, and *29* exhibited reduced expression under specific treatments, particularly drought and heat.

The expression patterns of *FaPINs* under salt, drought, cold, and heat stress, are consistent with the stress-induced responses observed in *PIN* gene families of other significant crop and model

plants. A number of *AtPINs* (most notably *AtPIN1, AtPIN3*, and *AtPIN7*) are increased in *Arabidopsis thaliana* under cold, drought, and salinity, suggesting their role in preserving auxin distribution and homeostasis during stress condition and facilitating hydrotropism and adaptive growth responses (Vieten, Sauer et al. 2007, Shibasaki, Uemura et al. 2009). In *Oryza sativa*, *OsPIN5c* and *OsPIN9* exhibit strong induction under salt and drought whereas heat stress results in considerable downregulation of several Os*PINs* (Manna, Rengasamy et al. 2022). Several *TaPIN* genes are activated under drought and heat, with *TaPIN8, 9* and *28* particularly responsive to combined heat and drought stress conditions (Kumar, Kherawat et al. 2021). In addition, many *PIN* genes in soybean (Wang, Chai et al. 2015), grapevine (Gou, Nai et al. 2022), maize (Yue, Tie et al. 2015, Li, Li et al. 2019), watermelon (Yu, Dong et al. 2017), pepper (Zhang, Dong et al. 2018) also showed significant differential expression in response to various abiotic stress conditions such as salt, drought, cold, heat and osmotic stress. These previous studies also highlight the functional significance of PIN genes under stress conditions, where they contribute to root elongation and auxin redistribution in rice, root plasticity and tiller formation in wheat, hydrotropic response and auxin homeostasis in *Arabidopsis*, fiber development and osmotic regulation in cotton, root system remodelling and maintenance of auxin transport in maize and enhanced auxin distribution and root growth in soybean. Collectively, these insights indicate that Fa*PIN* genes in strawberry are involved in regulating stress-responsive growth and developmental processes, performing distinct condition-specific roles that enable the plant to effectively adapt to various environmental challenges.

The hormonal treatment analysis demonstrated that *FaPIN* genes exhibit unique tissue-specific expression patterns, particularly in response to auxin and gibberellin signals. Under control condition, no significant difference between roots and leaves was observed; however, treatments with NAA, IAA, and GA_3 significantly increased FaPIN expression in roots. These treatments resulted in a significant upregulation of several genes, including *FaPIN3, 11, 13, 16, 18, 25*, and *27*, in roots compared to leaves. This suggests that auxin- and gibberellin-responsive regulation is primarily observed in root tissues. Comparative analysis reveals that the hormone-responsive expression patterns of FaPIN genes in strawberry align with those observed in other plant species. Auxin (IAA/NAA) substantially induces AtPIN1, AtPIN3, and AtPIN7 in *Arabidopsis thaliana*, promoting gravitropic responses and lateral root development (Paponov, Teale et al. 2005, Vieten, Sauer et al. 2007). Auxin and gibberellin treatments also result in increased expression of

OsPIN1b, OsPIN2 and *OsPIN5c* in *Oryza sativa* (rice), which aids in root elongation and shoot growth (Xu, Zhu et al. 2005, Wang, Hu et al. 2009, Li, Zhu et al. 2019). Fiber initiation and elongation are supported in *Gossypium hirsutum* (cotton) by the upregulation of *GhPIN1* and *GhPIN3* subsequent to the treatment of IAA and GA_3 (He, Zhao et al. 2017, Zhang, He et al. 2017). Root and shoot growth in *Zea mays* (maize) is regulated by *ZmPIN1a* and *ZmPIN9*, which react favorably to auxin and GA_3 (Forestan, Farinati et al. 2012, Yue, Tie et al. 2015, Li, Li et al. 2019). Under auxin and cytokinin, *TaPIN1a* and *TaPIN9* exhibit elevated expression in *Triticum aestivum* (wheat), which affects the growth of tillers and spikes (Kumar, Kherawat et al. 2021). Similarly, in *Vitis vinifera* (grapevine), auxin significantly induces *VvPIN1* and *VvPIN5*, which mediate organ differentiation and stress adaption (Gou, Nai et al. 2022) . These results collectively suggests that *FaPIN* genes are essential for maintaining auxin homeostasis and hormonal regulation in root development and signaling pathways

The presence of numerous *cis*-elements in the promoter regions of FaPIN genes further supports their potential involvement and regulatory roles in stress conditions and hormone treatments. These CREs reinforce the observed expression patterns and suggest a complex transcriptional regulation underlying *FaPIN*-mediated stress and hormone signaling pathways. Consequently, this gene family presents a promising target for future genetic engineering efforts aimed at improving strawberry productivity and enhancing tolerance to a broad spectrum of environmental stresses.

5. Conclusion

This research encompasses the comprehensive analysis of the PIN proteins in octoploid strawberry (*Fragaria x ananassa*) and their expression profiling under various abiotic stresses and hormonal treatments. Thirty *FaPIN* genes were identified across different chromosomes. The genes are classified into five distinct groups based on their phylogenetic tree. The identified *cis*-elements imply a functional role in regulating hormonal pathways, guiding developmental processes, and mediating response to wide range of stress-related stimuli. The role of *FaPIN* genes in abiotic stress responses and different hormone treatments was examined using RT-qPCR. Moreover, this study predicted the 3D structure of *FaPIN* proteins, offering structural insights into their functional mechanisms. These findings enhance our understanding of the biological roles of *FaPIN* genes in cultivated strawberry and provide a foundation for future research, potentially leading to genomic modifications aimed at furthering improvement and developing stress-tolerant varieties.

Acknowledgments

The authors gracefully acknowledge the financial and research support provided by the SUST Research Center and the Plant Genetic Engineering (PGE) Lab, Department of Genetic Engineering and Biotechnology at Shahjalal University of Science and Technology, Sylhet-3114, Bangladesh for conducting this research.

References

Adamowski, M. and J. Friml (2015). "PIN-dependent auxin transport: action, regulation, and evolution." The Plant Cell **27**(1): 20-32.

Anciro, A., J. Mangandi, S. Verma, N. Peres, V. M. Whitaker and S. Lee (2018). "FaRCg1: a quantitative trait locus conferring resistance to Colletotrichum crown rot caused by Colletotrichum gloeosporioides in octoploid strawberry." Theoretical and Applied Genetics **131**: 2167-2177.

Bailey, T. L. and C. Elkan (1994). "Fitting a mixture model by expectation maximization to discover motifs in bipolymers."

Bennett, T., S. F. Brockington, C. Rothfels, S. W. Graham, D. Stevenson, T. Kutchan, M. Rolf, P. Thomas, G. K.-S. Wong and O. Leyser (2014). "Paralogous radiations of PIN proteins with multiple origins of noncanonical PIN structure." Molecular Biology and Evolution **31**(8): 2042-2060.

Biovia, D. S. (2017). Discovery studio modeling environment, Release.

Blilou, I., J. Xu, M. Wildwater, V. Willemsen, I. Paponov, J. Friml, R. Heidstra, M. Aida, K. Palme and B. Scheres (2005). "The PIN auxin efflux facilitator network controls growth and patterning in Arabidopsis roots." Nature **433**(7021): 39-44.

Braybrook, S. A. (2019). Auxin and organogenesis: Initiation of organs and nurturing a scientific spirit, American Society of Plant Biologists. **31:** 1397-1397.

Chen, C., H. Chen, Y. Zhang, H. R. Thomas, M. H. Frank, Y. He and R. Xia (2020). "TBtools: an integrative toolkit developed for interactive analyses of big biological data." Molecular plant **13**(8): 1194-1202.

Colovos, C. and T. O. Yeates (1993). "Verification of protein structures: patterns of nonbonded atomic interactions." Protein science **2**(9): 1511-1519.

Deng, S., J. Sun, R. Zhao, M. Ding, Y. Zhang, Y. Sun, W. Wang, Y. Tan, D. Liu and X. Ma (2015). "Populus euphratica APYRASE2 enhances cold tolerance by modulating vesicular trafficking and extracellular ATP in Arabidopsis plants." Plant Physiology **169**(1): 530-548.

Deshmukh, R. K., H. Sonah and N. K. Singh (2016). "Intron gain, a dominant evolutionary process supporting high levels of gene expression in rice." Journal of Plant Biochemistry and Biotechnology **25**(2): 142-146.

Edger, P. P., T. J. Poorten, R. VanBuren, M. A. Hardigan, M. Colle, M. R. McKain, R. D. Smith, S. J. Teresi, A. D. Nelson and C. M. Wai (2019). "Origin and evolution of the octoploid strawberry genome." Nature genetics **51**(3): 541-547.

Estrella-Maldonado, H., G. Fuentes Ortiz, A. C. Chan Leon, L. C. Rodriguez Zapata, C. Talavera May, F. Espadas y Gil, F. Barredo Pool, F. M. Idrovo Espin and J. M. Santamaría (2016). "The papaya CpAUX1/LAX and CpPIN genes: Structure, phylogeny and expression analysis related to root formation on in vitro plantlets." Plant Cell, Tissue and Organ Culture (PCTOC) **126**(2): 187-204.

Forestan, C., S. Farinati and S. Varotto (2012). "The maize PIN gene family of auxin transporters." Frontiers in plant science **3**: 16.

Friml, J., J. Wiśniewska, E. Benková, K. Mendgen and K. Palme (2002). "Lateral relocation of auxin efflux regulator PIN3 mediates tropism in Arabidopsis." Nature **415**(6873): 806-809.

Ganguly, A., S. H. Lee, M. Cho, O. R. Lee, H. Yoo and H.-T. Cho (2010). "Differential auxin-transporting activities of PIN-FORMED proteins in Arabidopsis root hair cells." Plant physiology **153**(3): 1046-1061.

Gasteiger, E., C. Hoogland, A. Gattiker, S. e. Duvaud, M. R. Wilkins, R. D. Appel and A. Bairoch (2005). Protein identification and analysis tools on the ExPASy server, Springer.

Goodstein, D. M., S. Shu, R. Howson, R. Neupane, R. D. Hayes, J. Fazo, T. Mitros, W. Dirks, U. Hellsten and N. Putnam (2012). "Phytozome: a comparative platform for green plant genomics." Nucleic acids research **40**(D1): D1178-D1186.

Gou, H., G. Nai, S. Lu, W. Ma, B. Chen and J. Mao (2022). "Genome-wide identification and expression analysis of PIN gene family under phytohormone and abiotic stresses in Vitis Vinifera L." Physiology and Molecular Biology of Plants **28**(10): 1905-1919.

Grones, P. and J. Friml (2015). "Auxin transporters and binding proteins at a glance." Journal of Cell Science **128**(1): 1-7.

Guex, N. and M. C. Peitsch (1997). "SWISS-MODEL and the Swiss-Pdb Viewer: an environment for comparative protein modeling." electrophoresis **18**(15): 2714-2723.

Hazman, M., F. Kabil, S. Abd Elhamid and P. Nick (2020). "Double lysis: an integrative time-saving method yielding high-quality RNA from strawberry." Journal of Genetic Engineering and Biotechnology **18**: 1-8.

He, P., P. Zhao, L. Wang, Y. Zhang, X. Wang, H. Xiao, J. Yu and G. Xiao (2017). "The PIN gene family in cotton (Gossypium hirsutum): genome-wide identification and gene expression analyses during root development and abiotic stress responses." BMC genomics **18**(1): 507.

Heinig, M. and D. Frishman (2004). "STRIDE: a web server for secondary structure assignment from known atomic coordinates of proteins." Nucleic acids research **32**(suppl_2): W500-W502.

Horton, P., K.-J. Park, T. Obayashi, N. Fujita, H. Harada, C. Adams-Collier and K. Nakai (2007). "WoLF PSORT: protein localization predictor." Nucleic acids research **35**(suppl_2): W585-W587.

Hu, B., J. Jin, A.-Y. Guo, H. Zhang, J. Luo and G. Gao (2015). "GSDS 2.0: an upgraded gene feature visualization server." Bioinformatics **31**(8): 1296-1297.

Jain, M., A. Nijhawan, A. K. Tyagi and J. P. Khurana (2006). "Validation of housekeeping genes as internal control for studying gene expression in rice by quantitative real-time PCR." Biochemical and biophysical research communications **345**(2): 646-651.

Kim, D. E., D. Chivian and D. Baker (2004). "Protein structure prediction and analysis using the Robetta server." Nucleic acids research **32**(suppl_2): W526-W531.

Ko, J., H. Park, L. Heo and C. Seok (2012). "GalaxyWEB server for protein structure prediction and refinement." Nucleic acids research **40**(W1): W294-W297.

Koralewski, T. E. and K. V. Krutovsky (2011). "Evolution of exon-intron structure and alternative splicing." PloS one **6**(3): e18055.

Křeček, P., P. Skůpa, J. Libus, S. Naramoto, R. Tejos, J. Friml and E. Zažímalová (2009). "The PIN-FORMED (PIN) protein family of auxin transporters." Genome biology **10**: 1-11.

Křeček, P., P. Skůpa, J. Libus, S. Naramoto, R. Tejos, J. Friml and E. Zažímalová (2009). "The PIN-FORMED (PIN) protein family of auxin transporters." Genome biology **10**(12): 249.

Krogh, A., B. Larsson, G. Von Heijne and E. L. Sonnhammer (2001). "Predicting transmembrane protein topology with a hidden Markov model: application to complete genomes." Journal of molecular biology **305**(3): 567-580.

Kumar, M., B. S. Kherawat, P. Dey, D. Saha, A. Singh, S. K. Bhatia, G. S. Ghodake, A. A. Kadam, H.-U. Kim and S.-M. Chung (2021). "Genome-wide identification and characterization of PIN-FORMED (PIN) gene family reveals role in developmental and various stress conditions in Triticum aestivum L." International Journal of Molecular Sciences **22**(14): 7396.

Kumar, S., G. Stecher, M. Li, C. Knyaz and K. Tamura (2018). "MEGA X: molecular evolutionary genetics analysis across computing platforms." Molecular biology and evolution **35**(6): 1547.

Lamesch, P., T. Z. Berardini, D. Li, D. Swarbreck, C. Wilks, R. Sasidharan, R. Muller, K. Dreher, D. L. Alexander and M. Garcia-Hernandez (2012). "The Arabidopsis Information Resource (TAIR): improved gene annotation and new tools." Nucleic acids research **40**(D1): D1202-D1210.

Laskowski, R. A., J. A. C. Rullmann, M. W. MacArthur, R. Kaptein and J. M. Thornton (1996). "AQUA and PROCHECK-NMR: programs for checking the quality of protein structures solved by NMR." Journal of biomolecular NMR **8**: 477-486.

Lescot, M., P. Déhais, G. Thijs, K. Marchal, Y. Moreau, Y. Van de Peer, P. Rouzé and S. Rombauts (2002). "PlantCARE, a database of plant cis-acting regulatory elements and a portal to tools for in silico analysis of promoter sequences." Nucleic acids research **30**(1): 325-327.

Letunic, I. and P. Bork (2007). "Interactive Tree Of Life (iTOL): an online tool for phylogenetic tree display and annotation." Bioinformatics **23**(1): 127-128.

Li, Y., J. Zhu, L. Wu, Y. Shao, Y. Wu and C. Mao (2019). "Functional divergence of PIN1 paralogous genes in rice." Plant and Cell Physiology **60**(12): 2720-2732.

Li, Z., P. Li and J. Zhang (2019). "Expression analysis of PIN-formed auxin efflux transporter genes in maize." Plant Signaling & Behavior **14**(9): 1632689.

Liu, Y. and H. Wei (2017). "Genome-wide identification and evolution of the PIN-FORMED (PIN) gene family in Glycine max." Genome **60**(7): 564-571.

Livak, K. J. and T. D. Schmittgen (2001). "Analysis of relative gene expression data using real-time quantitative PCR and the 2− ΔΔCT method." methods **25**(4): 402-408.

Lu, S., J. Wang, F. Chitsaz, M. K. Derbyshire, R. C. Geer, N. R. Gonzales, M. Gwadz, D. I. Hurwitz, G. H. Marchler and J. S. Song (2020). "CDD/SPARCLE: the conserved domain database in 2020." Nucleic acids research **48**(D1): D265-D268.

MacIsaac, K. D. and E. Fraenkel (2006). "Practical strategies for discovering regulatory DNA sequence motifs." PLoS computational biology **2**(4): e36.

Manna, M., B. Rengasamy, N. K. Ambasht and A. K. Sinha (2022). "Characterization and expression profiling of PIN auxin efflux transporters reveal their role in developmental and abiotic stress conditions in rice." Frontiers in Plant Science **13**: 1059559.

Marand, A. P., A. L. Eveland, K. Kaufmann and N. M. Springer (2023). "cis-Regulatory elements in plant development, adaptation, and evolution." Annual review of plant biology **74**(1): 111-137.

Marhava, P., A. Bassukas, M. Zourelidou, M. Kolb, B. Moret, A. Fastner, W. Schulze, P. Cattaneo, U. Hammes and C. Schwechheimer (2018). "A molecular rheostat adjusts auxin flux to promote root protophloem differentiation." Nature **558**(7709): 297-300.

Mistry, J., S. Chuguransky, L. Williams, M. Qureshi, G. A. Salazar, E. L. Sonnhammer, S. C. Tosatto, L. Paladin, S. Raj and L. J. Richardson (2021). "Pfam: The protein families database in 2021." Nucleic acids research **49**(D1): D412-D419.

Miyashita, Y., T. Takasugi and Y. Ito (2010). "Identification and expression analysis of PIN genes in rice." Plant Science **178**(5): 424-428.

Monroy-González, Z., M. A. Uc-Chuc, A. O. Quintana-Escobar, F. Duarte-Aké and V. M. Loyola-Vargas (2023). "Characterization of the PIN Auxin Efflux Carrier Gene Family and Its Expression during Zygotic Embryogenesis in Persea americana." Plants **12**(12): 2280.

Motulsky, H. (1999). Analyzing Data with GraphPad Prism, GraphPad Software Incorporated.

Muthukumaran, J., P. Manivel, M. Kannan, J. Jeyakanthan and R. Krishna (2011). "A framework for classification of antifreeze proteins in over wintering plants based on their sequence and structural features." J. Bioinform. Seq. Anal **3**: 70-88.

Nagar, P., A. Kumar, M. Jain, S. Kumari and A. Mustafiz (2020). "Genome-wide analysis and transcript profiling of PSKR gene family members in Oryza sativa." PloS one **15**(7): e0236349.

Nicholas, K. B. (1997). "Genedoc: a tool for editing and annoting multiple sequence alignments." http://wwwpscedu/biomed/genedoc.

Njuguna, W., A. Liston, R. Cronn, T.-L. Ashman and N. Bassil (2013). "Insights into phylogeny, sex function and age of Fragaria based on whole chloroplast genome sequencing." Molecular Phylogenetics and Evolution **66**(1): 17-29.

Paponov, I. A., W. D. Teale, M. Trebar, I. Blilou and K. Palme (2005). "The PIN auxin efflux facilitators: evolutionary and functional perspectives." Trends in plant science **10**(4): 170-177.

Pattison, R. J. and C. Catalá (2012). "Evaluating auxin distribution in tomato (Solanum lycopersicum) through an analysis of the PIN and AUX/LAX gene families." The Plant Journal **70**(4): 585-598.

Perrot-Rechenmann, C. (2010). "Cellular responses to auxin: division versus expansion." Cold Spring Harbor perspectives in biology **2**(5): a001446.

Petrášek, J. and J. Friml (2009). "Auxin transport routes in plant development."

Potter, S. C., A. Luciani, S. R. Eddy, Y. Park, R. Lopez and R. D. Finn (2018). "HMMER web server: 2018 update." Nucleic acids research **46**(W1): W200-W204.

Retzer, K., M. Akhmanova, N. Konstantinova, K. Malínská, J. Leitner, J. Petrášek and C. Luschnig (2019). "Brassinosteroid signaling delimits root gravitropism via sorting of the Arabidopsis PIN2 auxin transporter." Nature communications **10**(1): 5516.

Robert, H. S., C. Park, C. L. Gutièrrez, B. Wójcikowska, A. Pěnčík, O. Novák, J. Chen, W. Grunewald, T. Dresselhaus and J. Friml (2018). "Maternal auxin supply contributes to early embryo patterning in Arabidopsis." Nature plants **4**(8): 548-553.

Shibasaki, K., M. Uemura, S. Tsurumi and A. Rahman (2009). "Auxin response in Arabidopsis under cold stress: underlying molecular mechanisms." The Plant Cell **21**(12): 3823-3838.

Shulaev, V., D. J. Sargent, R. N. Crowhurst, T. C. Mockler, O. Folkerts, A. L. Delcher, P. Jaiswal, K. Mockaitis, A. Liston and S. P. Mane (2011). "The genome of woodland strawberry (Fragaria vesca)." Nature genetics **43**(2): 109-116.

Sutoh, K. and D. Yamauchi (2003). "Two cis-acting elements necessary and sufficient for gibberellin-upregulated proteinase expression in rice seeds." The plant journal **34**(5): 635-645.

Tapia, R. R., C. R. Barbey, S. Chandra, K. M. Folta, V. M. Whitaker and S. Lee (2020). "Genome-wide identification and characterization of MLO gene family in octoploid strawberry (Fragaria× ananassa)." BioRxiv: 2020.2002. 2003.932764.

Teale, W. D., I. A. Paponov and K. Palme (2006). "Auxin in action: signalling, transport and the control of plant growth and development." Nature reviews Molecular cell biology **7**(11): 847-859.

Tian, R., J. Xu, Z. Xu, J. Li and H. Li (2024). "Genome-Wide identification and expression analysis of SWEET gene family in strawberry." Horticulturae **10**(2): 191.

Ung, K. L., M. Winkler, L. Schulz, M. Kolb, D. P. Janacek, E. Dedic, D. L. Stokes, U. Z. Hammes and B. P. Pedersen (2022). "Structures and mechanism of the plant PIN-FORMED auxin transporter." Nature **609**(7927): 605-610.

Vanneste, S. and J. Friml (2009). "Auxin: a trigger for change in plant development." Cell **136**(6): 1005-1016.

Velasquez, S. M., E. Barbez, J. Kleine-Vehn and J. M. Estevez (2016). "Auxin and cellular elongation." Plant physiology **170**(3): 1206-1215.

Viaene, T., C. F. Delwiche, S. A. Rensing and J. Friml (2013). "Origin and evolution of PIN auxin transporters in the green lineage." Trends in plant science **18**(1): 5-10.

Vieten, A., M. Sauer, P. B. Brewer and J. Friml (2007). "Molecular and cellular aspects of auxin-transport-mediated development." Trends in plant science **12**(4): 160-168.

Voorrips, R. (2002). "MapChart: software for the graphical presentation of linkage maps and QTLs." Journal of heredity **93**(1): 77-78.

Wang, J.-R., H. Hu, G.-H. Wang, J. Li, J.-Y. Chen and P. Wu (2009). "Expression of PIN genes in rice (Oryza sativa L.): tissue specificity and regulation by hormones." Molecular plant **2**(4): 823-831.

Wang, Y., C. Chai, B. Valliyodan, C. Maupin, B. Annen and H. T. Nguyen (2015). "Genome-wide analysis and expression profiling of the PIN auxin transporter gene family in soybean (Glycine max)." BMC genomics **16**(1): 951.

White, S. H. and W. C. Wimley (1999). "Membrane protein folding and stability: physical principles." Annual review of biophysics and biomolecular structure **28**(1): 319-365.

Wiederstein, M. and M. J. Sippl (2007). "ProSA-web: interactive web service for the recognition of errors in three-dimensional structures of proteins." Nucleic acids research **35**(suppl_2): W407-W410.

Wisniewska, J., J. Xu, D. Seifertová, P. B. Brewer, K. Ruzicka, I. Blilou, D. Rouquié, E. Benková, B. Scheres and J. Friml (2006). "Polar PIN localization directs auxin flow in plants." Science **312**(5775): 883-883.

Xu, M., L. Zhu, H. Shou and P. Wu (2005). "A PIN1 family gene, OsPIN1, involved in auxin-dependent adventitious root emergence and tillering in rice." Plant and cell physiology **46**(10): 1674-1681.

Ye, J., G. Coulouris, I. Zaretskaya, I. Cutcutache, S. Rozen and T. L. Madden (2012). "Primer-BLAST: a tool to design target-specific primers for polymerase chain reaction." BMC bioinformatics **13**: 1-11.

Yu, C., W. Dong, Y. Zhan, Z.-a. Huang, Z. Li, I. S. Kim and C. Zhang (2017). "Genome-wide identification and expression analysis of ClLAX, ClPIN and ClABCB genes families in Citrullus lanatus under various abiotic stresses and grafting." BMC genetics **18**(1): 33.

Yu, C. S., Y. C. Chen, C. H. Lu and J. K. Hwang (2006). "Prediction of protein subcellular localization." Proteins: Structure, Function, and Bioinformatics **64**(3): 643-651.

Yue, R., S. Tie, T. Sun, L. Zhang, Y. Yang, J. Qi, S. Yan, X. Han, H. Wang and C. Shen (2015). "Genome-wide identification and expression profiling analysis of ZmPIN, ZmPILS, ZmLAX and ZmABCB auxin transporter gene families in maize (Zea mays L.) under various abiotic stresses." PloS one **10**(3): e0118751.

Zhang, C., W. Dong, Z.-a. Huang, M. Cho, Q. Yu, C. Wu and C. Yu (2018). "Genome-wide identification and expression analysis of the CaLAX and CaPIN gene families in pepper (Capsicum annuum L.) under various abiotic stresses and hormone treatments." Genome **61**(2): 121-130.

Zhang, Y., P. He, Z. Yang, G. Huang, L. Wang, C. Pang, H. Xiao, P. Zhao, J. Yu and G. Xiao (2017). "A genome-scale analysis of the PIN gene family reveals its functions in cotton fiber development." Frontiers in plant science **8**: 461.

Zhao, Y. (2010). "Auxin biosynthesis and its role in plant development." Annual review of plant biology **61**(1): 49-64.

List of Figures

Fig. 1. Prediction of transmembrane regions for *Fragaria x ananassa* FaPIN proteins using TMHHM v.2.0 M software (transmembrane prediction using hidden Markov models). The predicted transmembrane domains are shown in purple, regions on the cytoplasmic side are indicated in blue, and regions outside are marked in orange.

Fig. 2. Phylogenetic investigation of PIN proteins in *Fragaria x ananassa*, *Oryza sativa*, *Arabidopsis thaliana* and *Fragaria vesca*. Maximum-likelihood method with 1000 bootstrap replicates was used to construct the tree in MEGA X. The tree was clustered into five major groups depicted in different colors.

Fig. 3. Gene structure analysis of *FaPIN* gene family. Black lines represent introns and yellow boxes represent exons. Blue boxes are used to symbolize untranslated regions (UTRs). The scale below can be used to estimate the lengths of exons and introns.

Fig. 4. Conserved motifs of FaPINs. The motifs are depicted by 15 different colored boxes. Protein sequence consensus for the corresponding motif is displayed in the legends below.

Fig. 5. Chromosomal distribution of *FaPIN* genes in *F.* × *ananassa*. The Figure was generated via MapChart. Chromosome numbers are labeled at the top, and gene position are shown relative to the scale on the left.

Fig. 6 Schematic depiction of hormonal-regulation and stress-responsive CREs in *FaPINs*. The scale at the bottom depicts the nucleotides upstream of the translation start site. Distinct colors denote distinct CREs. Abiotic stress-responsive: GC-motif, ARE, LTR, MBS, CCAAT-box, DRE core, MYB, MYB-recognition site, MYC, and STRE. Biotic stress-responsive: W box, WRE3, and WUN-motif. Hormonal regulation: ABRE, ABRE3a, ABRE4, ABRE2, GARE-motif, p-box, TCA, TCA-element, TGA-element, CARE, CGTCA-motif, TGACG-motif, ERE, as-1, TATC-box, and AuxRR-core

Fig. 7. Secondary structure analysis of FaPIN proteins. STRIDE program was used to generate the structure. Legend of secondary structure icons are shown at the bottom-right corner.

Fig. 8. Predicted 3D structures of FaPIN proteins. The tertiary structures were constructed by Robetta online server, and then Biovia Discovery Studio Visualizer was used to visualize them.

Fig. 9. Relative expression profiling of *FaPIN* genes in response to different abiotic stress conditions determined by RT-qPCR. The relative expression value of each *FaPIN* in the leaves of plant is shown on the Y-axis, and the X-axis denotes the different stress treatmnets. Mean value of expression at each stress treatment was determined via technical replication. Data were analyzed in GraphPad Prism 9.0.0 and Microsoft Office 2019. One-way ANOVA and Bonferroni post-hoc test were performed to determine the significant difference ($P \leq 0.05$). To show the significant differences, different means were labeled with different numbers of stars (*).

Fig. 10. Relative expression of the *FaPIN* genes in leaf and root tissues under various hormonal treatments by determined RT-qPCR. Legend: Black columns indicate expression in leaf and gray

columns indicate expression in root tissue. The X-axis represents the hormonal treatments (Control, NAA, IAA and GA3) and the Y-axis indicates the relative expression level. Abbreviation: IAA- indole-3-aceric acid; GA3- gibberellin; NAA- 1-naphthaleneacetic acid. Mean value of expression at each treatment was determined via technical replication. Data were analyzed in GraphPad Prism 9.0.0 and Microsoft Office 2019. Two-way ANOVA and Bonferroni post-hoc test were performed to determine the significant difference ($P \leq 0.05$). To show the significant differences, different means were labeled with different numbers of stars (*).

List of Tables

Table 1. Characteristics of the *PIN* gene family in *Fragaria x ananassa*.

Supplementary File Information

Fig. S1. Multiple Sequence Alignment of FaPIN protein sequences. The alignment shows conserved amino acid regions across the 30 FaPIN proteins, highlighting typical PIN structures including transmembrane domains at both termini and a central hydrophilic loop. Conserved motifs suggest functional similarity among family members.

Fig. S2. Ramachandran plots of the predicted tertiary structures of FaPIN proteins. The plots were generated using the PROCHECK server. Residues are distributed across regions indicated by different colors- red for the most favored, yellow for additionally allowed, pale yellow for generously allowed, and white for disallowed conformations, illustrating the stereochemical quality of the modeled structures.

Fig. S3. ProSA-web Z-score plots of the FaPIN protein models. Structural validation was performed using the ProSA-web tool, which calculates Z-scores to assess overall model quality. Light blue zones indicate the Z-score range for proteins solved by X-ray crystallography, and dark blue denotes those determined by NMR spectroscopy. Each black dot represents a FaPIN model, with all scores falling within the acceptable range for native-like structures.

File S1. ERRAT quality plots of the predicted tertiary structures of FaPIN proteins. The plots were generated using the ERRAT server to evaluate non-bonded atomic interactions. Yellow regions

indicate segments of the protein structure that may be rejected at a 95 % confidence level, red regions at a 99 % confidence level, while white regions represent areas with fewer errors, suggesting higher structural reliability.

Table. S1 Domain organization of *FaPIN* genes predicted using pfam and HMMSCAN with default parameters.

Table. S2 List of identified *cis*-regulatory elements in the 5′ UTR region of *FaPIN*s by using PlantCARE database.

Table. S3 Secondary structure analysis of the FaPIN members in cultivated strawberry

Table. S4 Tertiary structure validation score of FaPIN proteins via different tools.

Table. S5 List of *FaPIN* primers used in this study

Table 1. Characteristics of the PIN gene family in Fragaria x ananassa.

Gene Name	Gene ID	Transcript ID	Chr. No	Location	Strand	Gene length (bp)	cDNA (bp)	CDS (bp)	Protein (aa)	MW (KDa)	pI	II	GRAVY Value	Subcellular localization
FaPIN1	maker-Fvb1-1-snap-gene-135.24	maker-Fvb1-1-snap-gene-135.24-mRNA-1	Fvb1-1	13583544-13588985	Forward	5441	1767	1767	588	65.27	5.49	44.65	0.047	Plas[ab]
FaPIN2	augustus_masked-Fvb1-3-processed-gene-127.13	augustus_masked-Fvb1-3-processed-gene-127.13-mRNA-1	Fvb1-3	12754102-12755278	Reverse	1176	1176	1176	391	43.26	9.84	48.65	0.011	Plas[ab]
FaPIN3	augustus_masked-Fvb1-4-processed-gene-52.7	augustus_masked-Fvb1-4-processed-gene-52.7-mRNA-1	Fvb1-4	5248630-5249980	Forward	1350	1191	1191	396	42.34	4.65	35.38	0.307	Plas[ab]
FaPIN4	augustus_masked-Fvb2-2-processed-gene-116.3	augustus_masked-Fvb2-2-processed-gene-116.3-mRNA-1	Fvb2-2	11603765-11604707	Forward	942	942	942	313	35.01	6.91	38.24	0.305	Plas[ab]
FaPIN5	maker-Fvb4-1-augustus-gene-45.24	maker-Fvb4-1-augustus-gene-45.24-mRNA-1	Fvb4-1	4570732-4573054	Forward	2322	1263	1263	420	45.33	9.47	48.1	0.359	Plas[ab]
FaPIN6	maker-Fvb4-1-augustus-gene-46.17	maker-Fvb4-1-augustus-gene-46.17-mRNA-1	Fvb4-1	4601585-4604830	Forward	3245	2458	1941	646	69.81	9.16	41.64	0.187	Plas[ab]
FaPIN7	maker-Fvb4-1-augustus-gene-180.31	maker-Fvb4-1-augustus-gene-180.31-mRNA-1	Fvb4-1	17999670-18003921	Reverse	4251	3132	1989	662	72.07	7.77	36.94	0.091	Plas[ab]
FaPIN8	maker-Fvb4-2-augustus-gene-24.29	maker-Fvb4-2-augustus-gene-24.29-mRNA-1	Fvb4-2	2395360-2399675	Forward	3021	3187	1989	662	72.06	7.76	36.97	0.1	Plas[ab]
FaPIN9	maker-Fvb4-2-snap-gene-203.31	maker-Fvb4-2-snap-gene-203.31-mRNA-1	Fvb4-2	20309968-20323595	Reverse	13627	4154	3744	1247	135.05	9.26	44.66	0.133	Plas[ab]
FaPIN10	maker-Fvb4-3-augustus-gene-26.32	maker-Fvb4-3-augustus-gene-26.32-mRNA-1	Fvb4-3	2655588-2659811	Forward	4223	3000	1989	662	72.11	7.77	35.22	0.104	Plas[ab]
FaPIN11	maker-Fvb4-3-snap-gene-271.29	maker-Fvb4-3-snap-gene-271.29-mRNA-1	Fvb4-3	27092860-27095572	Forward	2712	1818	1818	605	65.69	8.23	46.78	0.294	Plas[ab]
FaPIN12	augustus_masked-Fvb4-3-processed-gene-271.2	augustus_masked-Fvb4-3-processed-gene-271.2-mRNA-1	Fvb4-3	27105587-27109068	Forward	3481	2392	1923	640	69.19	9.04	43.07	0.153	Plas[ab]
FaPIN13	maker-Fvb4-4-augustus-gene-25.34	maker-Fvb4-4-augustus-gene-25.34-mRNA-1	Fvb4-4	2559756-2564014	Forward	4258	3119	1989	662	72.19	7.76	36.64	0.103	Plas[ab]
FaPIN14	maker-Fvb4-4-augustus-gene-241.22	maker-Fvb4-4-augustus-gene-241.22-mRNA-1	Fvb4-4	24094251-24097472	Reverse	3221	2436	1938	645	69.82	9.19	43.44	0.142	Plas[ab]
FaPIN15	maker-Fvb4-4-augustus-gene-241.25	maker-Fvb4-4-augustus-gene-241.25-mRNA-1	Fvb4-4	24132894-24136211	Reverse	3317	2555	1311	436	47.72	6.81	48.34	0.022	Plas[ab]
FaPIN16	maker-Fvb5-1-augustus-gene-106.31	maker-Fvb5-1-augustus-gene-106.31-mRNA-1	Fvb5-1	10633685-10637735	Forward	4050	2948	1983	660	72.35	9.36	35.48	-0.01	Plas[ab]
FaPIN17	snap_masked-Fvb5-2-processed-gene-98.23	snap_masked-Fvb5-2-processed-gene-98.23-mRNA-1	Fvb5-2	9869627-9873426	Forward	3799	2730	1641	546	59.81	7.71	36.66	-0.173	Plas[ab]
FaPIN18	maker-Fvb5-3-augustus-gene-182.59	maker-Fvb5-3-augustus-gene-182.59-mRNA-1	Fvb5-3	18203516-18207362	Reverse	3846	2762	1956	651	71.25	9.43	36.96	-0.011	Plas[ab]
FaPIN19	maker-Fvb5-4-augustus-gene-78.39	maker-Fvb5-4-augustus-gene-78.39-mRNA-1	Fvb5-4	7815064-7818969	Forward	3905	2771	2010	669	73.44	9.42	35.34	-0.055	Plas[ab]
FaPIN20	maker-Fvb6-1-augustus-gene-32.61	maker-Fvb6-1-augustus-gene-32.61-mRNA-1	Fvb6-1	3271778-3273647	Reverse	1869	1139	1074	357	38.7	9.33	39.55	0.632	Vacu[a] Plas[b]
FaPIN21	maker-Fvb6-1-augustus-gene-138.40	maker-Fvb6-1-augustus-gene-138.40-mRNA-1	Fvb6-1	13863283-13864633	Reverse	1350	1254	1254	417	44.56	5.04	37.39	0.22	Plas[ab]
FaPIN22	maker-Fvb6-1-augustus-gene-357.42	maker-Fvb6-1-augustus-gene-357.42-mRNA-1	Fvb6-1	35700321-35702919	Reverse	2598	1413	1074	357	39.27	6.51	35.63	0.807	Vacu[a] Plas[b]
FaPIN23	maker-Fvb6-2-augustus-gene-269.44	maker-Fvb6-2-augustus-gene-269.44-mRNA-1	Fvb6-2	26895936-26898504	Forward	2568	1373	1074	357	39.27	6.51	35.63	0.807	Vacu[a] Plas[b]
FaPIN24	maker-Fvb6-2-augustus-gene-302.55	maker-Fvb6-2-augustus-gene-302.55-mRNA-1	Fvb6-2	30219908-30221713	Reverse	1805	1074	1074	357	38.7	9.33	39.55	0.632	Vacu[a] Plas[b]
FaPIN25	maker-Fvb6-3-snap-gene-27.59	maker-Fvb6-3-snap-gene-27.59-mRNA-1	Fvb6-3	2736828-2738705	Reverse	1877	1141	1074	357	38.79	9.33	38.12	0.634	Plas[ab]
FaPIN26	maker-Fvb6-3-augustus-gene-187.14	maker-Fvb6-3-augustus-gene-187.14-mRNA-1	Fvb6-3	18736174-18739195	Reverse	3021	2311	1731	576	62.68	9.32	33.66	0.27	Plas[ab]
FaPIN27	maker-Fvb6-3-augustus-gene-426.43	maker-Fvb6-3-augustus-gene-426.43-mRNA-1	Fvb6-3	42679921-42682664	Forward	2743	1512	1074	357	39.24	6.51	39.64	0.769	Vacu[a] Plas[b]
FaPIN28	maker-Fvb6-4-augustus-gene-26.69	maker-Fvb6-4-augustus-gene-26.69-mRNA-1	Fvb6-4	2681441-2683996	Reverse	2555	1050	1050	349	38.33	7.56	36.21	0.707	Vacu[a] Plas[b]
FaPIN29	maker-Fvb6-4-augustus-gene-184.29	maker-Fvb6-4-augustus-gene-184.29-mRNA-1	Fvb6-4	18469590-18473493	Reverse	3903	2750	1731	576	62.5	9.09	34.31	0.257	Plas[ab]
FaPIN30	maker-Fvb6-4-augustus-gene-341.84	maker-Fvb6-4-augustus-gene-341.84-mRNA-1	Fvb6-4	34177080-34178971	Forward	1891	1136	1074	357	38.67	9.33	39.75	0.636	Vacu[a] Plas[b]

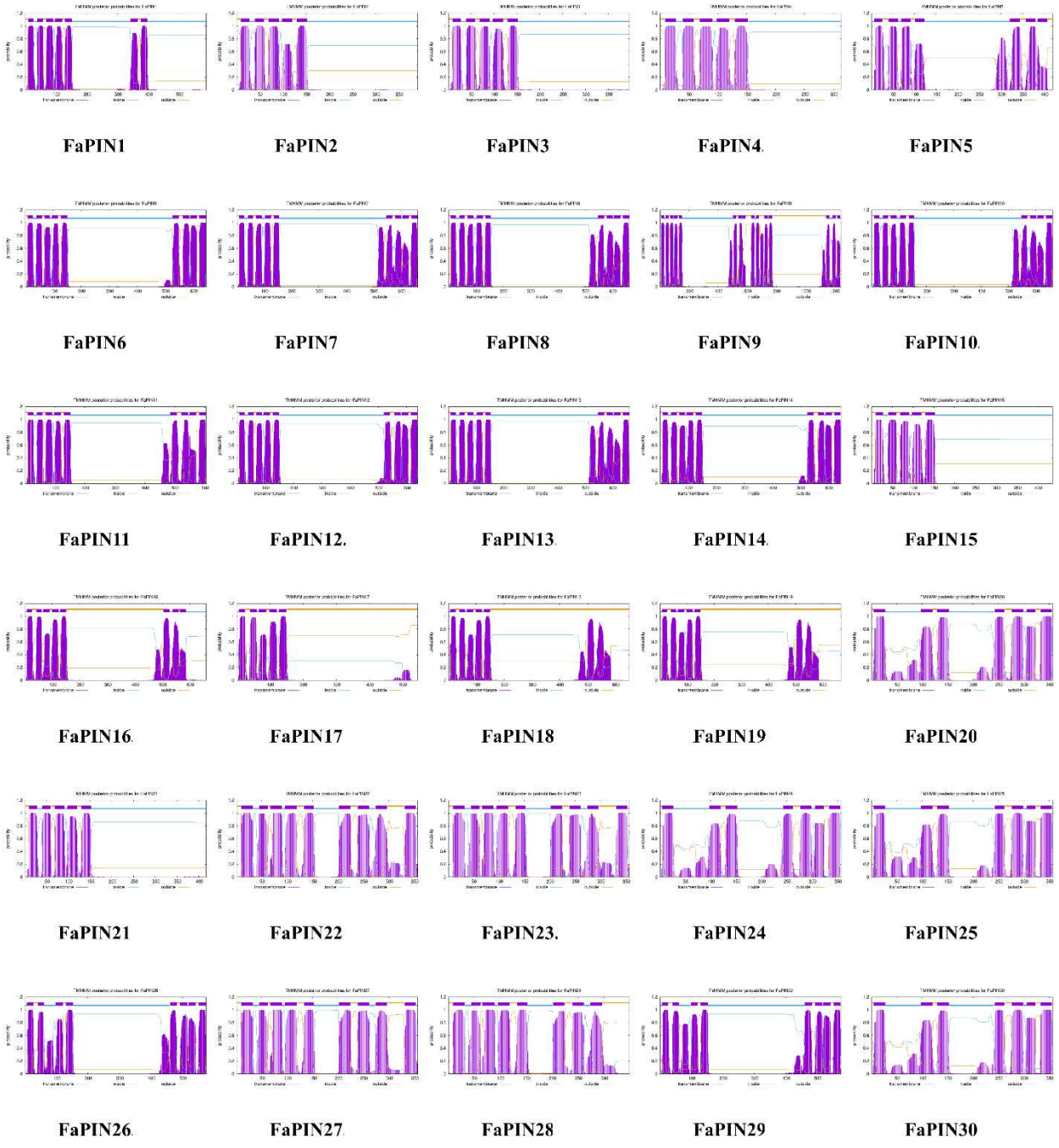

FaPIN1
FaPIN2
FaPIN3
FaPIN4
FaPIN5
FaPIN6
FaPIN7
FaPIN8
FaPIN9
FaPIN10
FaPIN11
FaPIN12
FaPIN13
FaPIN14
FaPIN15
FaPIN16
FaPIN17
FaPIN18
FaPIN19
FaPIN20
FaPIN21
FaPIN22
FaPIN23
FaPIN24
FaPIN25
FaPIN26
FaPIN27
FaPIN28
FaPIN29
FaPIN30

Figure 1

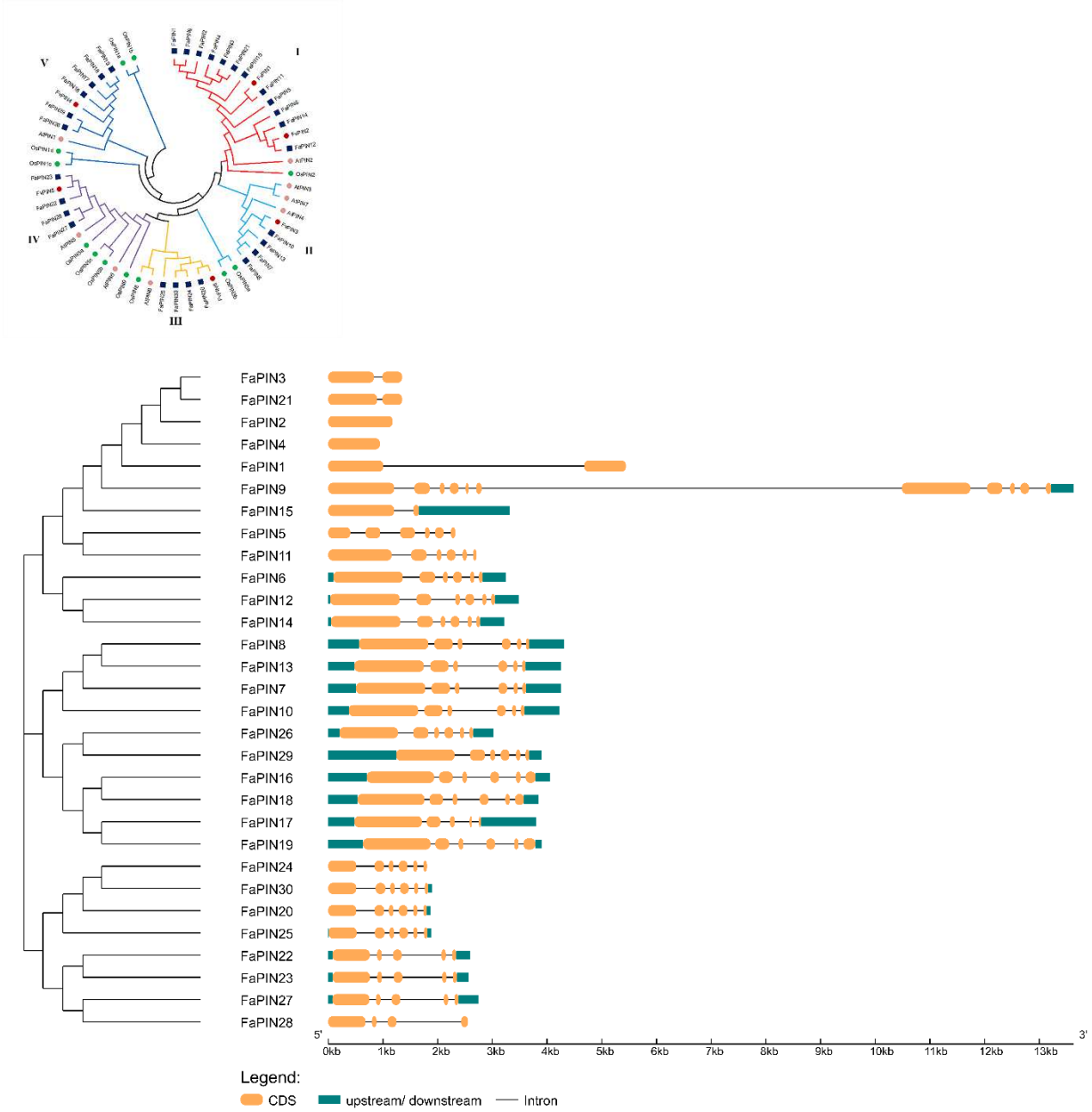

I
II
III
IV
V
FaPIN3
FaPIN21
FaPIN2
FaPIN4
FaPIN1
FaPIN9
FaPIN15
FaPIN5
FaPIN11
FaPIN6
FaPIN12
FaPIN14
FaPIN8
FaPIN13
FaPIN7
FaPIN10
FaPIN26
FaPIN29
FaPIN16
FaPIN18
FaPIN17
FaPIN19
FaPIN24
FaPIN30
FaPIN20
FaPIN25
FaPIN22
FaPIN23
FaPIN27
FaPIN28
5'
3'
0kb
1kb
2kb
3kb
4kb
5kb
6kb
7kb
8kb
9kb
10kb
11kb
12kb
13kb
Legend:
CDS
upstream/ downstream
Intron

Figure 2

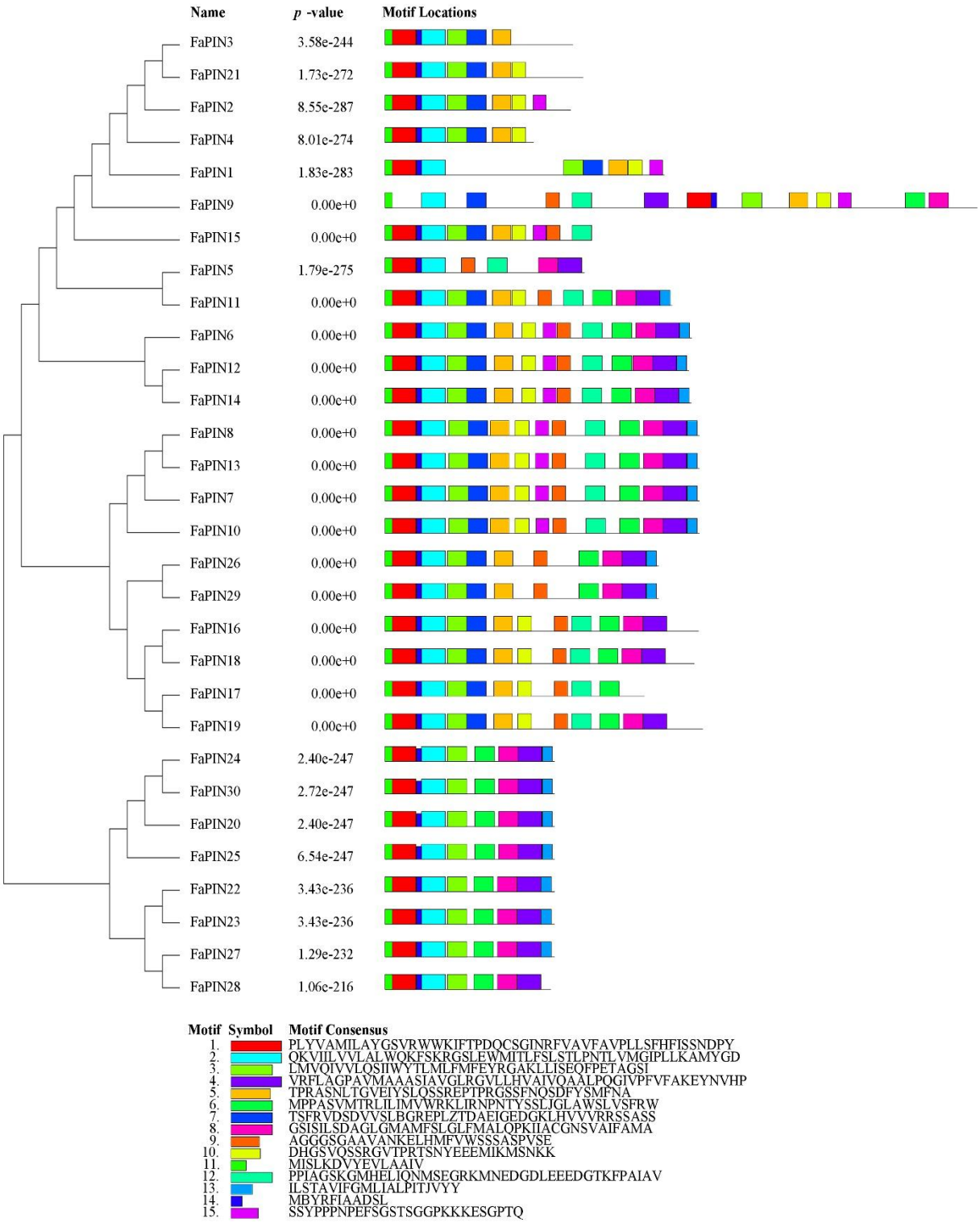

Name
p -value
Motif Locations
FaPIN3 3.58e-244
FaPIN21 1.73e-272
FaPIN2 8.55e-287
FaPIN4 8.01e-274
FaPIN1 1.83e-283
FaPIN9 0.00e+0
FaPIN15 0.00e+0
FaPIN5 1.79e-275
FaPIN11 0.00e+0
FaPIN6 0.00e+0
FaPIN12 0.00e+0
FaPIN14 0.00e+0
FaPIN8 0.00e+0
FaPIN13 0.00e+0
FaPIN7 0.00e+0
FaPIN10 0.00e+0
FaPIN26 0.00e+0
FaPIN29 0.00e+0
FaPIN16 0.00e+0
FaPIN18 0.00e+0
FaPIN17 0.00e+0
FaPIN19 0.00e+0
FaPIN24 2.40e-247
FaPIN30 2.72e-247
FaPIN20 2.40e-247
FaPIN25 6.54e-247
FaPIN22 3.43e-236
FaPIN23 3.43e-236
FaPIN27 1.29e-232
FaPIN28 1.06e-216
Motif Symbol
Motif Consensus
1. PLYVAMILAYGSVRWWKIFTPDQCSGINRFVAVFAVPLLSFHFISSNDPY
2. QKVIILVVLALWQKFSKRGSLEWMITLFSLSTLPNTLVMGIPLLKAMYGD
3. LMVQIVVLQSIIWYTLMLFMFEYRGAKLLISEQFPETAGSI
4. VRFLAGPAVMAAASIAVGLRGVLLHVAIVQAALPQGIVPFVFAKEYNVHP
5. TPRASNLTGVEIYSLQSSREPTPRGSSFNQSDFYSMFNA
6. MPPASVMTRLILIMVWRKLIRNPNTYSSLIGLAWSLVSFRW
7. TSFRVDSDVVSLBGREPLZTDAEIGEDGKLHVVVRRSSASS
8. GSISILSDAGLGMAMFSLGLFMALQPKIIACGNSVAIFAMA
9. AGGGSGAAVANKELHMFVWSSSASPVSE
10. DHGSVQSSRGVTPRTSNYEEEMIKMSNKK
11. MISLKDVYEVLAAIV
12. PPIAGSKGMHELIQNMSEGRKMNEDGDLEEEDGTKFPAIAV
13. ILSTAVIFGMLIALPITJVYY
14. MBYRFIAADSL
15. SSYPPPNPEFSGSTSGGPKKKESGPTQ

Figure 3

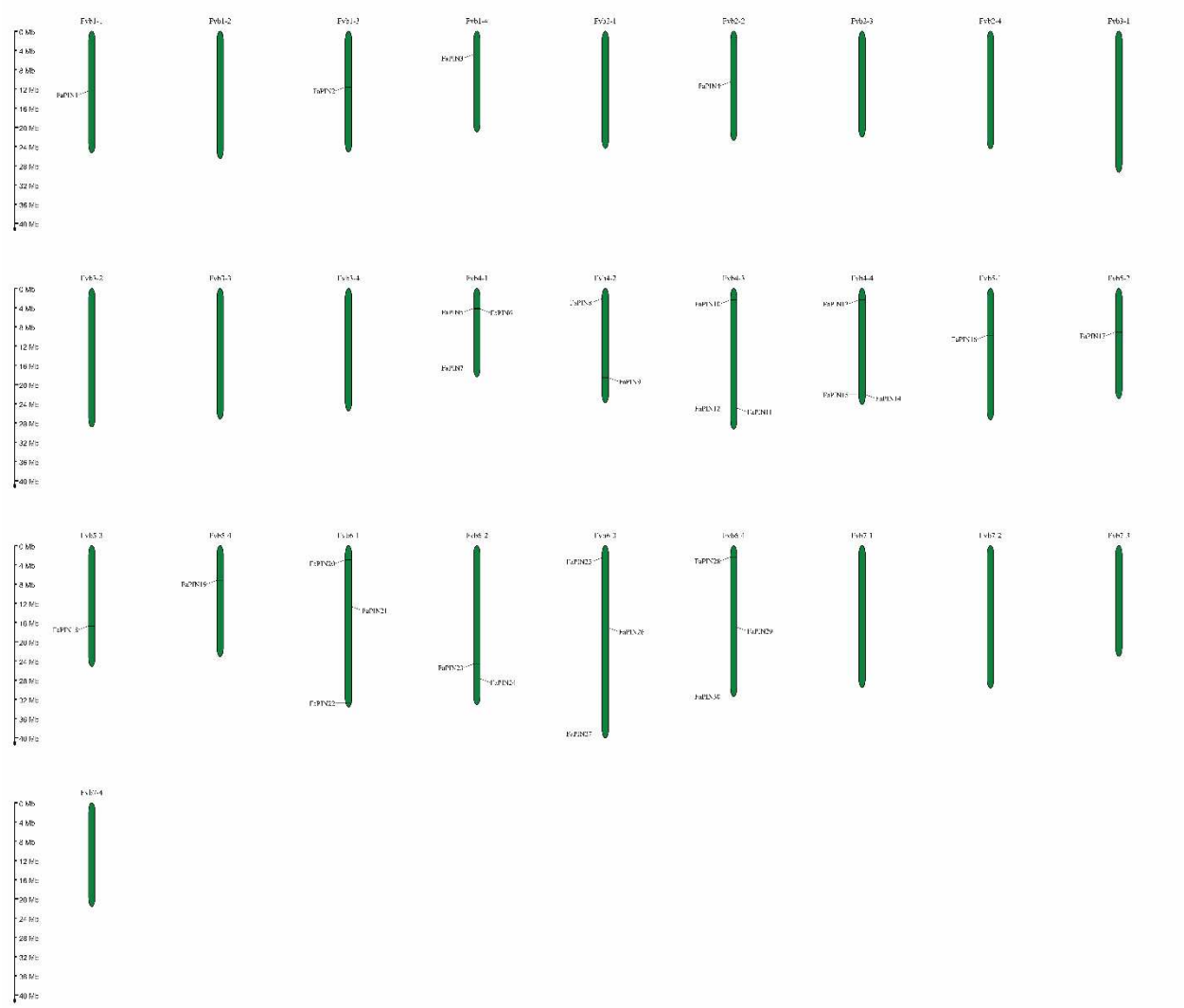


Figure 4

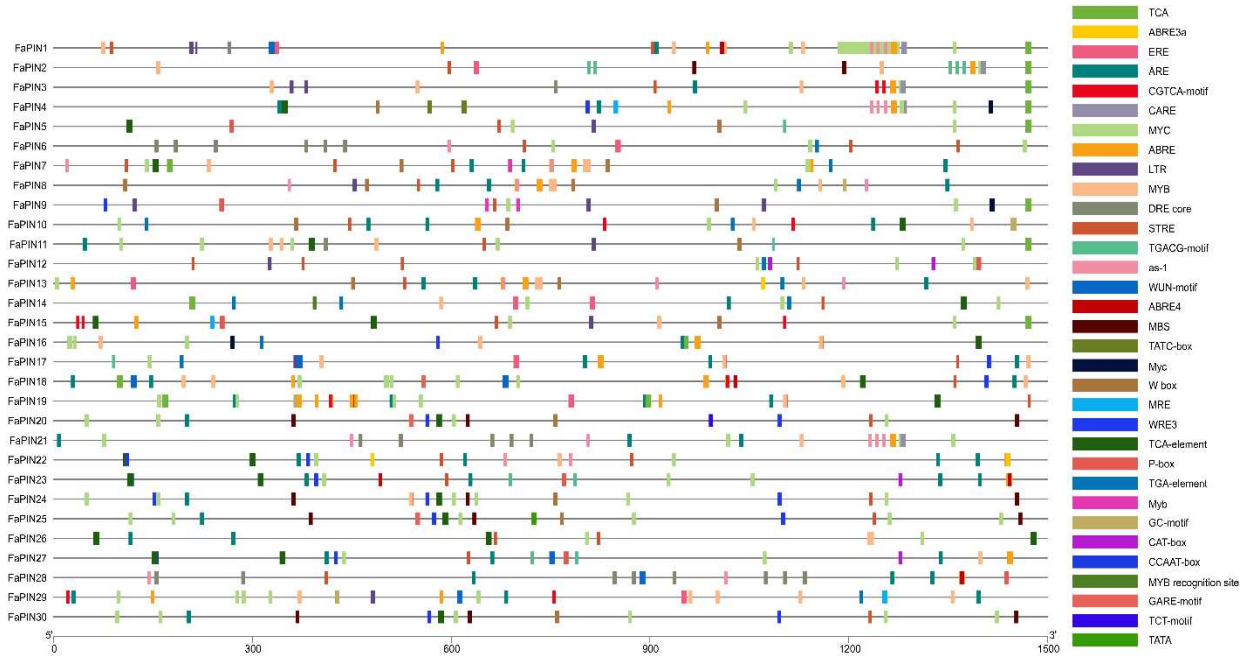

FaPIN1
FaPIN2
FaPIN3
FaPIN4
FaPIN5
FaPIN6
FaPIN7
FaPIN8
FaPIN9
FaPIN10
FaPIN11
FaPIN12
FaPIN13
FaPIN14
FaPIN15
FaPIN16
FaPIN17
FaPIN18
FaPIN19
FaPIN20
FaPIN21
FaPIN22
FaPIN23
FaPIN24
FaPIN25
FaPIN26
FaPIN27
FaPIN28
FaPIN29
FaPIN30
5'
3'
0
300
600
900
1200
1500
TCA
ABRE3a
ERE
ARE
CGTCA-motif
CARE
MYC
ABRE
LTR
MYB
DRE core
STRE
TGACG-motif
as-1
WUN-motif
ABRE4
MBS
TATC-box
Myc
W box
MRE
WRE3
TCA-element
P-box
TGA-element
Myb
GC-motif
CAT-box
CCAAT-box
MYB recognition site
GARE-motif
TCT-motif
TATA

Figure 5

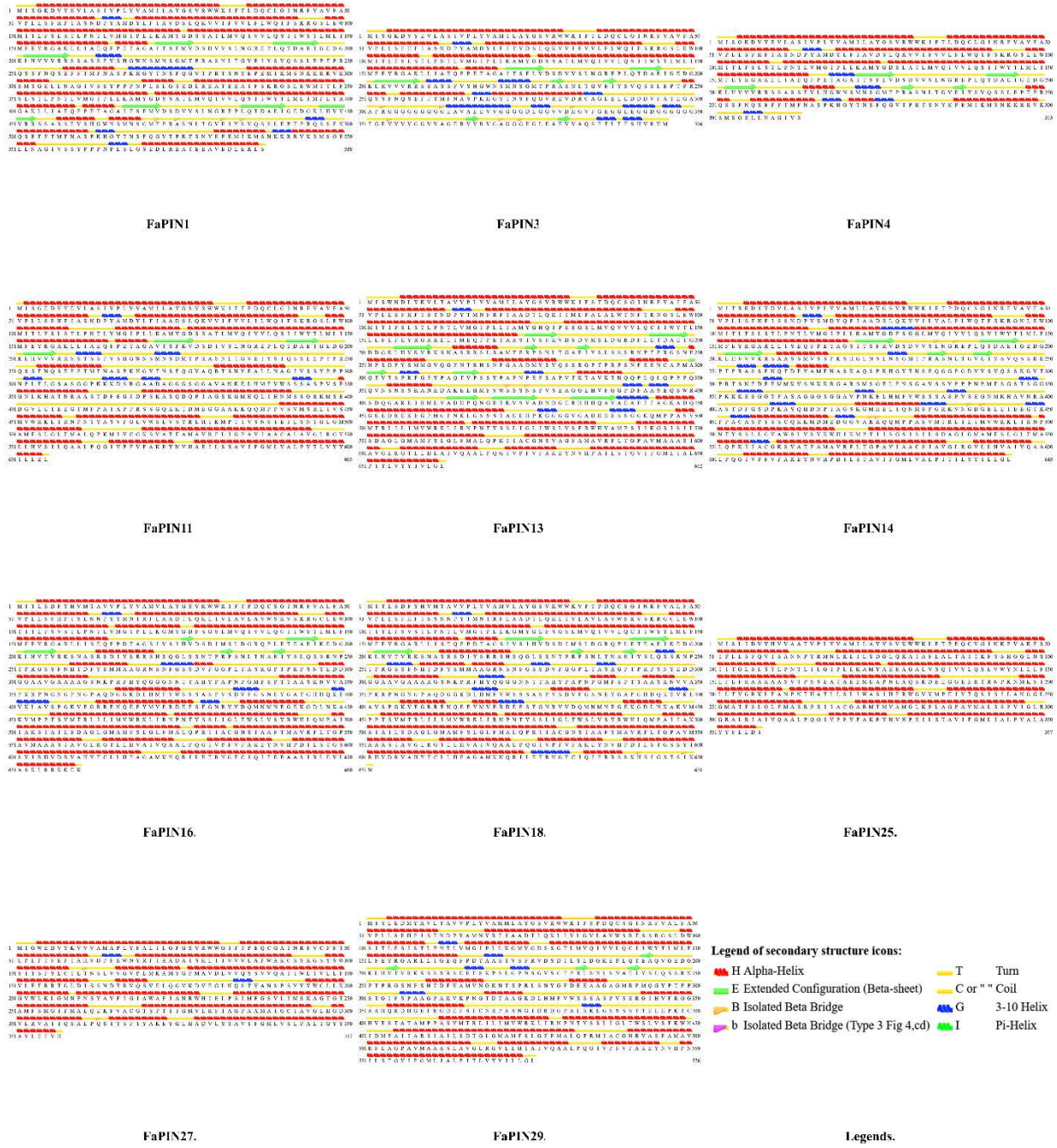

FaPIN1
FaPIN3
FaPIN4
FaPIN11
FaPIN13
FaPIN14
FaPIN16.
FaPIN18.
FaPIN25.
FaPIN27.
FaPIN29.
Legends.
Legend of secondary structure icons:
H Alpha-Helix
E Extended Configuration (Beta-sheet)
B Isolated Beta Bridge
b Isolated Beta Bridge (Type 3 Fig 4,cd)
T Turn
C or " " Coil
G 3-10 Helix
I Pi-Helix

Figure 6

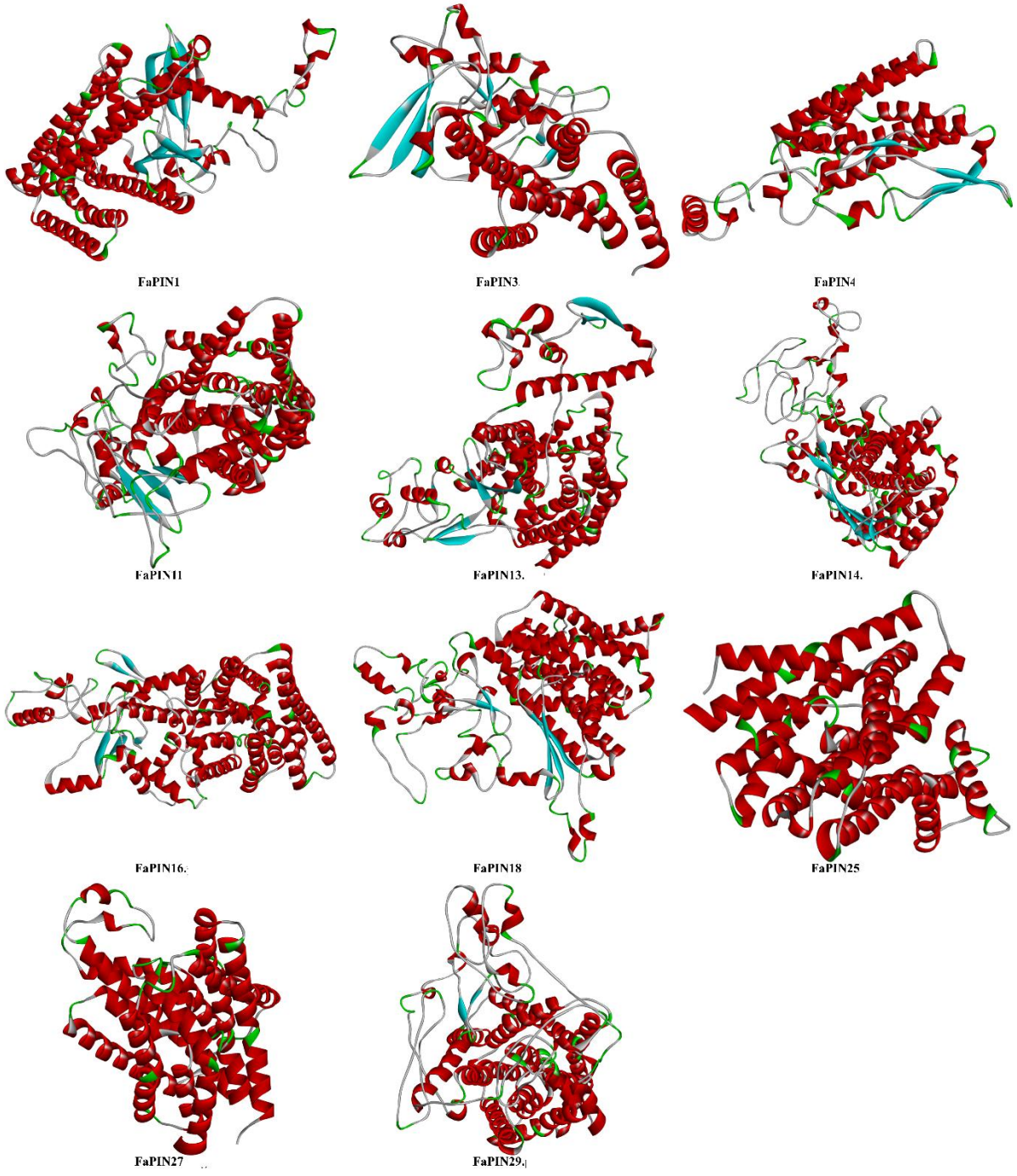

FaPIN1
FaPIN3
FaPIN4
FaPIN11
FaPIN13.
FaPIN14.
FaPIN16.
FaPIN18
FaPIN25
FaPIN27
FaPIN29.

Figure 7

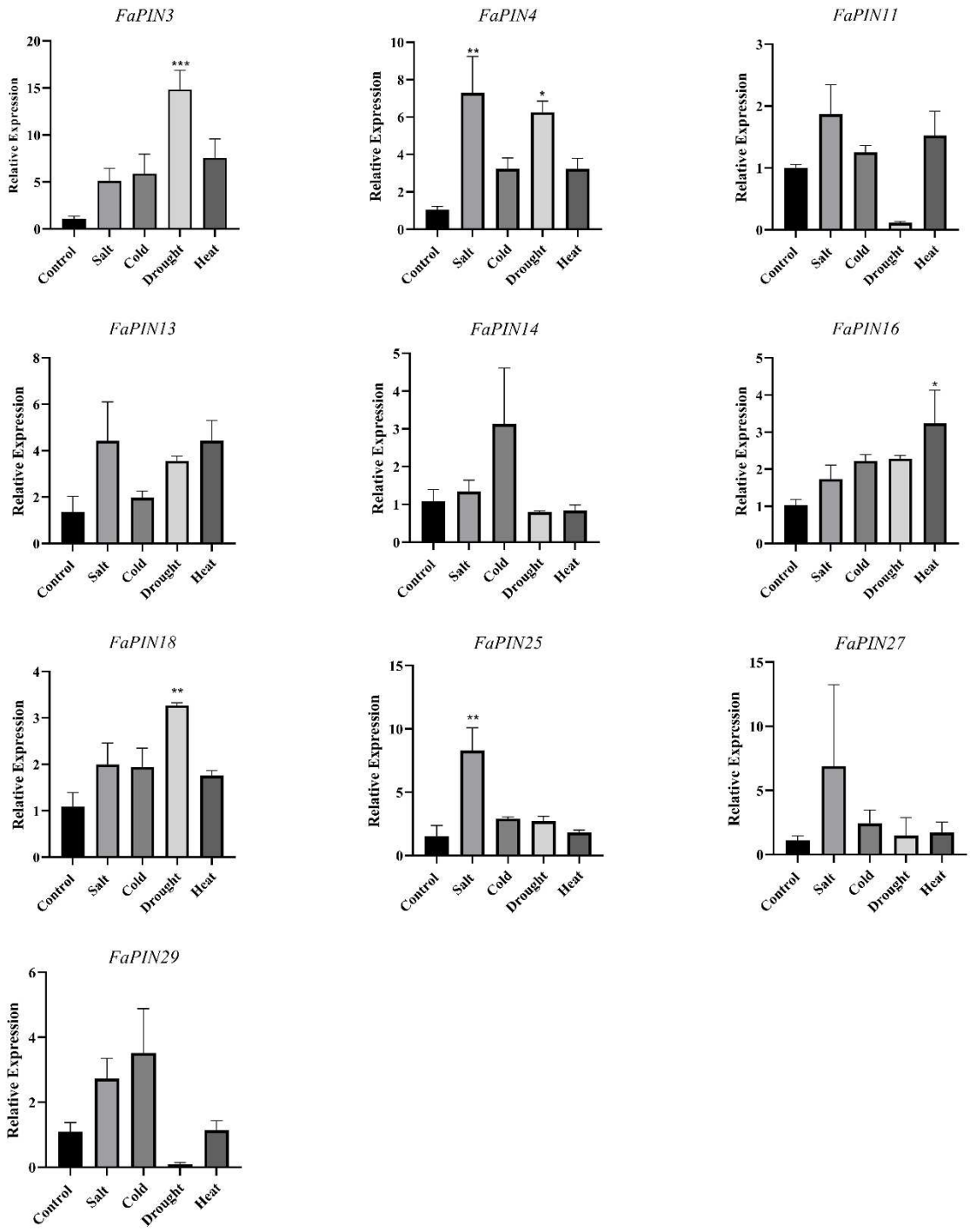

FaPIN3
FaPIN4
FaPIN11
FaPIN13
FaPIN14
FaPIN16
FaPIN18
FaPIN25
FaPIN27
FaPIN29
Relative Expression
Control
Salt
Cold
Drought
Heat

Figure 8

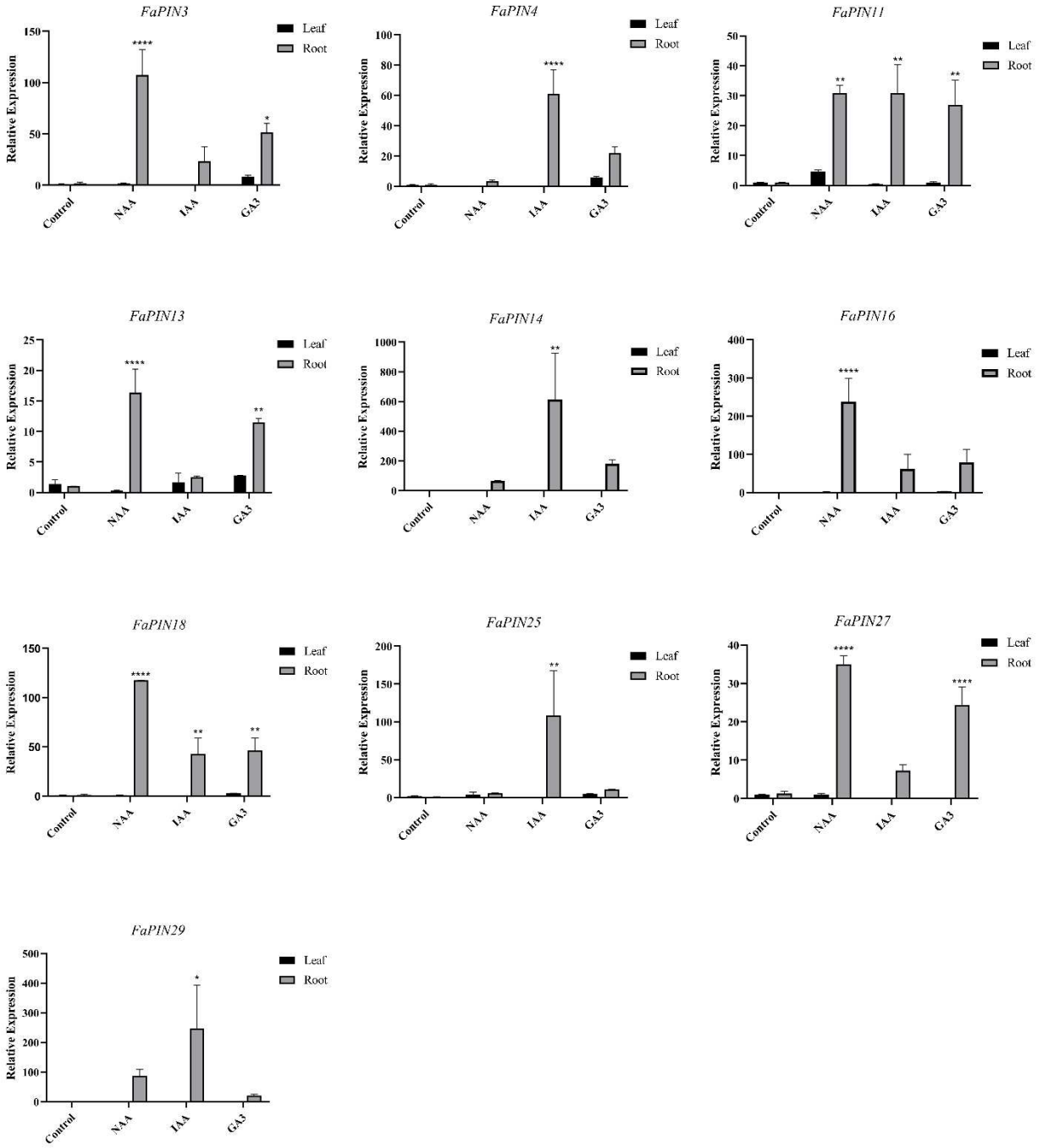

FaPIN3
FaPIN4
FaPIN11
FaPIN13
FaPIN14
FaPIN16
FaPIN18
FaPIN25
FaPIN27
FaPIN29
Relative Expression
Leaf
Root
Control
NAA
IAA
GA3

Figure 9